

An efficient solution procedure for solving higher-codimension Hopf and Bogdanov-Takens bifurcations[†]

Bing Zeng^a, Pei Yu^b, Maoan Han^{c,*}

^a*School of Mathematics and Statistics, Lingnan Normal University,
Zhanjiang, Guandong, 524048, China*

^b*Department of Mathematics, Western University,
London, Ontario, N6A 5B7, Canada*

^c*Department of Mathematics, Zhejiang Normal University,
Jinhua, Zhejiang, 321004, China*

Abstract

In solving real world systems for higher-codimension bifurcation problems, one often faces the difficulty in computing the normal form or the focus values associated with generalized Hopf bifurcation, and the normal form with unfolding for higher-codimension Bogdanov-Takens bifurcation. The difficulty is not only coming from the tedious symbolic computation of focus values, but also due to the restriction on the system parameters, which frequently leads to failure of the conventional approach used in the computation even for simple 2-dimensional nonlinear dynamical systems. In this paper, we use a simple 2-dimensional epidemic model, for which the conventional approach fails in analyzing the stability of limit cycles arising from Hopf bifurcation, to illustrate how our method can be efficiently applied to determine the codimension of Hopf bifurcation. Further, we apply the simplest normal form theory to consider codimension-3 Bogdanov-Takens bifurcation and present an efficient one-step transformation approach, compared with the classical six-step transformation approach to demonstrate the advantage of our method.

Keywords: Generalized Hopf bifurcation, Bogdanov-Takens (B-T) bifurcation, hierarchical parametric analysis, codimension, limit cycle, the simplest normal form.

2000 MSC: 34C07, 34C15

*Corresponding author

Email addresses: zengbing969@163.com (Bing Zeng), pyu@uwo.ca (Pei Yu), mahan@zjnu.edu.cn (Maoan Han)

[†]The first draft of this article has been posted on arXiv.org since August 28, 2022, No. 2208.13228v1.

1. Introduction

Limit cycle theory plays a very important role in the study of nonlinear dynamical systems, related to the well-known phenomenon of self-oscillations arising from physical science and engineering [8, 11]. Hopf and Bogdanov-Takens (B-T) bifurcations are two main bifurcations generating limit cycles in real world systems. A common task of the study in such systems is to determine the codimension of the bifurcation and to derive the associated normal form, which is not easy for higher-codimension bifurcations. Particularly, when considering practical systems, determining the codimension of the two bifurcations becomes very difficult due to physical limitations on the system parameters. For example, consider the maximal number of limit cycles arising from generalized Hopf bifurcation in a 2-dimensional nonlinear system, which may be reduced from an n -dimensional system by applying center manifold theory, described by the following ordinary differential equations:

$$\dot{x} = f(x, \mu, \alpha), \quad x \in \mathbb{R}^2, \quad \mu \in \mathbb{R}, \quad \alpha \in \mathbb{R}^m, \quad (1)$$

where the dot denotes differentiation with respect to time t , μ is a perturbation parameter, and α is a constant vector representing the coefficients or parameters in the function f . Assume that $x = 0$ is an equilibrium of (1), yielding $f(0, \mu, \alpha) = 0$. Moreover, suppose that the Jacobian of the system evaluated on the equilibrium $x = 0$ at the critical point $\mu = \mu_c = 0$ has a pair of purely imaginary eigenvalues $\pm i\omega_c$. Then, applying the normal form theory (e.g. see [8, 11, 12, 15, 17]) to (1), associated with the Hopf bifurcation, we obtain the following *classical/conventional* normal form (CNF) in the polar coordinates,

$$\begin{aligned} \dot{r} &= r(v_0 + v_1 r^2 + v_2 r^4 + \dots + v_k r^{2k} + \dots), \\ \dot{\theta} &= \omega_c + \tau_0 \mu + \tau_1 r^2 + \tau_2 r^4 + \dots + \tau_k r^{2k} + \dots, \end{aligned} \quad (2)$$

where r and θ are the amplitude and phase of motion, respectively, v_j ($j = 0, 1, 2, \dots$) is called the j th-order focus value. Note that v_j 's are functions of α and μ . v_0 is obtained from a linear analysis as $v_0 = v_H \mu$, where $v_H \neq 0$ is called the transversal condition of Hopf bifurcation, while finding v_j ($j \geq 1$) needs a nonlinear analysis such as normal form or focus value computation. Note that the frequency ω_c is usually scaled to 1.

The CNF can be further simplified to the so called *simplest normal form* (SNF) or *unique/minimal normal form* or *hypernormal form* (e.g. see [1, 2, 5–7, 18, 20–22]). The SNF of Hopf bifurcation can be classified into three categories (at the Hopf critical point

with $\mu = 0$, i.e., $v_0 = 0$) [20] as follows:

$$\begin{aligned}
\text{(I)} \quad v_1 \neq 0: & \quad \begin{cases} \dot{r} = v_1 \rho^3 + v_2 \rho^5, \\ \dot{\theta} = 1 + \tau_1 \rho^2; \end{cases} \\
\text{(II)} \quad \begin{cases} v_1 = v_2 = \cdots = v_{k-1} = 0, v_k \neq 0 \\ \tau_1 = \tau_2 = \cdots = \tau_{k-1} = 0 \end{cases} : & \quad \begin{cases} \dot{r} = v_k \rho^{2k+1} + v_{2k} \rho^{4k+1}, \\ \dot{\theta} = 1 + \tau_k \rho^{2k}; \end{cases} \\
\text{(III)} \quad \begin{cases} v_1 = v_2 = \cdots = v_{k-1} = 0, v_k \neq 0 \\ \tau_1 = \tau_2 = \cdots = \tau_{j-2} = 0, \tau_{j-1} \neq 0, (1 \leq j \leq k) \end{cases} : & \quad \begin{cases} \dot{r} = v_k \rho^{2k+1} + v_{2k} \rho^{4k+1}, \\ \dot{\theta} = 1 + \tau_{j-1} \rho^{2(j-1)} + \tau_j \rho^{2j} + \cdots + \tau_k \rho^{2k}. \end{cases}
\end{aligned} \tag{3}$$

It can be seen that the CNF (2) contains an infinite number of “tails”, while the SNF (3) has only a finite number of terms, since the infinite tails in the CNF have been removed by a further arbitrarily high-order nonlinear transformation. Then, the codimension of Hopf bifurcation is defined by the first non-vanishing focus value. Thus, the codimension of Hopf bifurcation is 1 for the case (I), and k for the cases (II) and (III). However, it should be noted that the above conclusion is based on the assumption that the vector parameter α is real (without any additional restriction), and therefore the number k can usually reach its maximal value.

In solving Hopf bifurcation problems, the standard approach is to compute the focus values (or the normal form) of the system associated with a Hopf bifurcation from an equilibrium solution. The computation is often carried out with the aid of a computer algebraic software such as Maple or Mathematica. Then, one needs to solve a multivariate polynomial system based on the normal form or the focus values. There are two main difficulties in dealing with the problems related to the above normal forms. The first one is due to the symbolic computational complexity in the focus value (or the normal form) computation, which is a result of the application of the conventional approach used in stability and bifurcation analysis. This will be seen in the next section when we deal with Hopf bifurcation in a simple epidemic model. The second difficulty is owing to that practical systems often have extra restriction on the system parameters because system parameters must be positive or even restricted to certain limited values. Suppose that the system under consideration involves 4 real parameters. In general, if these parameters are assumed real, then the maximal number of bifurcating limit cycles may be 4, the same as the number of parameters. However, if it is a biological system

or other physical systems, due to limitation on the parameters, the maximal number of limit cycles might be 3, 2, or even only 1. In this case, determining the codimension of the Hopf bifurcation, that is, determining the maximal number of bifurcating limit cycles can be much more difficult. The difficulty is mainly from solving the polynomial systems (suppose the focus values have been obtained), since one needs to determine the sign of the polynomials with the variation of many variables (parameters).

For the Bogdanov-Takens (B-T) bifurcation, the analysis of codimension-2 B-T bifurcation has become standard [8, 12]. However, for codimension-3 or higher-codimension (or degenerate) B-T bifurcations, the computation of the normal forms becomes much more involved, particularly in order to establish the relation between the original system and the simplified system (the normal form). Consider the system (1) which now has a nilpotent critical point at the origin (characterized by a double-zero eigenvalue), with more than one perturbation parameters (unfolding), which is rewritten as

$$\dot{x} = f(x, \mu, \alpha), \quad x \in \mathbb{R}^2, \quad \mu \in \mathbb{R}^p, \quad (p \geq 2), \quad \alpha \in \mathbb{R}^m, \quad (4)$$

Then, the CNF of B-T bifurcation for system (4) at the critical point $\mu=0$ can be written as (e.g., see [8, 11, 12, 17])

$$\begin{aligned} \dot{x}_1 &= x_2, \\ \dot{x}_2 &= \sum_{k=2}^{\infty} (c_{k0} x_1^k + c_{(k-1)1} x_1^{k-1} x_2), \end{aligned} \quad (5)$$

where the normal form coefficients c_{k0} and $c_{(k-1)1}$ are functions of the vector parameter α and μ . Unlike the SNF of Hopf bifurcation, the classification of the SNF of (4) is much more complicated. The most common case in real applications is the cusp B-T bifurcation and degenerate cusp B-T bifurcations when $c_{20} \neq 0$. The SNF for such B-T bifurcations is given by [9, 22]

$$\begin{aligned} \dot{x}_1 &= x_2, \\ \dot{x}_2 &= c_{20} x_1^2 + c_{11} x_1 x_2 + c_{31} x_1^3 x_2 + c_{41} x_1^4 x_2 + c_{61} x_1^6 x_2 + c_{71} x_1^7 x_2 + \dots \end{aligned} \quad (6)$$

which can be used to estimate the codimension of the B-T bifurcation. Besides the case $c_{20} \neq 0$, the first non-vanishing coefficients determines the codimension. For example, it is a codimension-2 (cusp) B-T bifurcation when $c_{11} \neq 0$; a codimension-3 (degenerate cusp) B-T bifurcation when $c_{11} = 0$ and $c_{31} \neq 0$; and a codimension-4 (degenerate cusp) B-T bifurcation when $c_{11} = c_{31} = 0$ and $c_{41} \neq 0$; and so on. In general, the first non-vanishing

coefficient can be written as c_{j1} , where $j = \lceil \frac{3(k-1)}{2} \rceil$, ($k \geq 2$). However, whether or not such an estimate of the codimension is true depends upon the derivation of the unfolding expressed in the perturbation parameters. This leads to much more computational demanding and will be seen in section 3.

The codimension-3 degenerate cusp B-T bifurcation (when $c_{20}c_{31} \neq 0$, $c_{11} = 0$) was studied by Dumortier *et al.* in 1987 [4], and the classical six-step transformation approach was developed and widely used by researchers in deriving the SNF with unfolding. We remark that some mistakes appeared in discussing B-T bifurcation in [4], and were pointed out and corrected in [10]. Recently, the so-called one-step transformation method was proposed [22, 23], which provides the transformation for the state variables, the parameters and the time rescaling in just one step, yielding a direct relation between the original system and the SNF. This not only greatly simplifies the analysis, but also clearly shows the impact of the original system parameters on the dynamical behaviours of the system. This method is based on the SNF theory and the parametric simplest normal (PSNF) theory [5–7, 20–22]. The key step involved in this method is to choose appropriate bases for the SNF and PSNF, as well as in the nonlinear transformations.

In nowadays, using computer software package such as MATCONT [3] or XPPAUTO [16] to plot bifurcation diagrams of nonlinear dynamical systems becomes very popular and quite useful in applications, particularly for lower-codimension bifurcations such as saddle-node, transcritical, Hopf and B-T bifurcations. The basic idea is to use computer simulation to search the critical bifurcation points/curves in the parameter space, and the bifurcation diagram is usually plotted in a 2-dimensional parameter plane. However, such techniques do not provide analytical formulas in terms of parameters for a parametric study in designs. Also, they are not applicable for higher-codimension bifurcations. Therefore, it is necessary to develop efficient methods for the analysis of higher-codimension bifurcations.

In this paper, we will use a simple epidemic model to illustrate how to determine the codimension of Hopf and B-T bifurcations. In particular, we will show how to determine the codimension of Hopf bifurcation, and introduce both the six-step and one-step transformation approaches for the codimension-3 (degenerate cusp) B-T bifurcation to give a comparison. The epidemic model has been studied in [14] for Hopf bifurcation and codimension-2 B-T bifurcation. Later, Li *et al.* [13] gave a complete analysis on the codimension-3 B-T bifurcation using the six-step method. The simple SI-epidemic model

is described by the following differential equations,

$$\begin{aligned}\frac{dS}{dt} &= A - dS - \beta(1 + \varepsilon I)SI, \\ \frac{dI}{dt} &= \beta(1 + \varepsilon I)SI - (d + \alpha)I,\end{aligned}\tag{7}$$

where S and I represent the numbers of the susceptible and infective populations, respectively; A , d and α denote the recruitment rate of susceptibles, the nature death rate, and the sum of the recover rate and the disease-related death rate, respectively; and $\beta(1 + \varepsilon I)SI$ is the incidence rate. All the parameters A , d , α , β and ε take positive real values.

In [14], the authors use $I = X$, $N = S + I = Y$ and apply the rescaling $\tau = \alpha t$ to model (7) to obtain the following dimensionless system,

$$\begin{aligned}\frac{dX}{d\tau} &= X [k(1 + \varepsilon X)(Y - X) - (n + 1)], \\ \frac{dY}{d\tau} &= m - nY - X,\end{aligned}\tag{8}$$

where the new parameters are defined as

$$k = \frac{\beta}{\alpha}, \quad m = \frac{A}{\alpha}, \quad n = \frac{d}{\alpha}.\tag{9}$$

Later, this model was further studied by Zeng and Yu [24] for a detailed analysis on Hopf bifurcation. Note that the dimensionless model (8) contains 4 parameters. However, one can make a further transformation, as given by

$$X = mx, \quad Y = my, \quad k = \frac{1}{m} \kappa, \quad \varepsilon = \frac{1}{m} e,\tag{10}$$

to eliminate the parameter m , yielding

$$\begin{aligned}\frac{dx}{d\tau} &= x [\kappa(1 + ex)(y - x) - (n + 1)], \\ \frac{dy}{d\tau} &= 1 - ny - x.\end{aligned}\tag{11}$$

In other words, under the transformation (10), without loss of generality, one can simply set $m = 1$ in system (8). In this paper, we will use system (11) for bifurcation analysis. In fact, using the system (8) shows that m does not play any roles on the bifurcation analysis. However, in order to keep our simulation results consistent with those given in

[14] and [24], our simulations presented in this paper are still based on system (8), and all the notations introduced later for system (11) can be easily extended to system (8) with the transformation (10).

It should be pointed out that most epidemic models have the well-posedness property, that is, solutions of such a model remain positive if the initial points take positive values, and are bounded. However, for the system (11) (or the system (8)), the first quadrant in the x - y plane is not invariant. Trajectories starting from the initial points in the first quadrant may pass through the x -axis to enter the fourth quadrant and then return to the first quadrant. Since the y -axis is invariant, any trajectories starting from the initial points in the first or fourth quadrant will either remain in or eventually enter the first quadrant. In other words, if restricted to the region: $\{(x, y) \mid x \geq 0\}$, the well-posedness property on the solutions of (8) is well defined. Although this model is not perfect, we do not intend to improve it since the aim of this paper is to use this model to demonstrate a solution procedure for studying higher-codimension Hopf and B-T bifurcations. As discussed in [14], we may focus on the domain of interest for the model, defined by

$$\begin{aligned} \Omega &= \left\{ (x, y) \mid 0 \leq x < y \leq \frac{1}{n} \right\} && \text{for system (11),} \\ \text{or } \Omega &= \left\{ (X, Y) \mid 0 \leq X < Y \leq \frac{m}{n} \right\} && \text{for system (8).} \end{aligned} \tag{12}$$

Note that Ω does not serve as a trapping region for the dynamical solutions in the first quadrant.

In the next section, we study Hopf and generalized Hopf bifurcations of system (11) and focus on the study of codimension. Then, in Section 3 we consider the B-T bifurcation in system (11) and pay particular attention to codimension-3 B-T bifurcation. Various simulations showing different bifurcation phenomena are given to illustrate the theoretical predictions. A concluding remark is given in Section 4.

2. Hopf bifurcation of system (11)

In this section, we first derive the equilibrium solutions of system (11) and their stability, and then consider the maximal number of limit cycles which may bifurcate from Hopf critical points. Although the stability conditions for the equilibria of system (8) were given in [14], the analysis on Hopf bifurcation has not been completely explored. In particular, we will rigorously prove that the codimension of the Hopf bifurcation is two. When using a classical method, one usually expresses equilibrium solutions in terms

of the system parameters. The advantage of this approach is to show the dynamical behaviours of the system, such as stability and bifurcations, clearly in the parameter space. However, if the equilibrium solutions cannot be simply expressed in terms of the system parameters, for example, if they are determined by a quadratic equation, then the analysis on stability and bifurcations becomes much more involved. Especially, it causes more difficulty in computing normal forms (focus values) and it is almost impossible to determine whether a focus value can change its sign or not, which is directly related to determining the codimension of Hopf bifurcation.

2.1. Stability of bifurcating limit cycles

First, we derive the conditions for the existence of the equilibrium solutions of system (11) and their stability. We will give a complete partition in the parameter space for the bifurcation analysis. Setting $\frac{dx}{d\tau} = \frac{dy}{d\tau} = 0$ in system (11) yields two equilibrium solutions,

$$\begin{aligned} P_0 : (x_0, y_0) &= \left(0, \frac{1}{n}\right), \\ P_1 : (x_1, y_1) &= \left(1 - ny_1, y_1\right), \quad \left(0 < y_1 < \frac{1}{n}\right), \end{aligned} \quad (13)$$

where P_0 is the infection-free equilibrium (boundary equilibrium) and P_1 is the infectious equilibrium (positive equilibrium), with y_1 determined from the following quadratic polynomial,

$$g(y_1, \kappa) = 1 + \kappa e n (y_1 - y_{1*})(y_1 - y_1^*), \quad \text{where } y_{1*} = \frac{1}{n+1}, \quad y_1^* = \frac{1}{n} + \frac{1}{en}. \quad (14)$$

Solving $g = 0$ gives the infectious equilibrium solutions,

$$y_{1\pm} = \frac{1}{2\kappa e n(n+1)} \left\{ \kappa [e(2n+1) + n + 1] \pm \sqrt{\Delta} \right\}, \quad x_{1\pm} = 1 - ny_{1\pm}, \quad (15)$$

where

$$\Delta = \kappa [\kappa (e + n + 1)^2 - 4en(n+1)^2]. \quad (16)$$

For convenience, define

$$\begin{aligned}
P_{1\pm} &= (1 - n y_{1\pm}, y_{1\pm}), \\
e_1 &= n + 1, \quad e_2 = 4n e_1^2, \quad e_3 = \frac{e_1^2}{1 - n}, \quad (n < 1), \quad e_4 = \frac{e_1^2}{n}, \\
e_{\pm} &= \frac{e_1}{2n} \left[n + 1 \pm \sqrt{(n + 1)(1 - 3n)} \right], \quad \left(n \leq \frac{1}{3} \right), \\
\kappa_T &= n e_1, \quad \kappa_{SN} = \frac{e e_2}{(e + e_1)^2}, \quad \kappa^* = \frac{2n e e_1 e_4}{(e + e_1)(e + e_4)}, \\
\kappa_{H\pm} &= \frac{e [n(e + e_4) + e] \pm n(e_4 - e) \sqrt{e(e - e_2)}}{2(e + e_1)^2}, \\
y_{1SN} &= \frac{1}{e_1} + \frac{1}{2n} \left(\frac{1}{e} + \frac{1}{e_1} \right) \in (y_{1*}, y_1^*), \quad y_{1T} = \frac{1}{n} \in (y_{1*}, y_1^*), \\
R_0 &= \frac{\kappa}{n(n + 1)} \triangleq \frac{\kappa}{\kappa_T},
\end{aligned} \tag{17}$$

where R_0 is the basic reproduction number, and the subscripts T, SN and H represent Transcritical, Saddle-node and Hopf bifurcations. All the above notations for y_1 , e and κ can be similarly defined for Y_1 , ε and k of system (8) via the transformation (10) as follows:

$$\begin{aligned}
Y_{1\pm} &= m y_{1\pm}, \quad Y_{1SN} = m y_{1SN}, \quad Y_{1T} = m y_{1T}, \quad Y_{1*} = m y_{1*}, \quad Y_1^* = m y_1^* \\
\varepsilon_i &= \frac{e_i}{m}, \quad i = 1, 2, 3, 4, \quad \varepsilon_{\pm} = \frac{e_{\pm}}{m}, \\
k_T &= \frac{\kappa_T}{m}, \quad k_{SN} = \frac{\kappa_{SN}}{m}, \quad k^* = \frac{\kappa^*}{m}, \quad k_{H\pm} = \frac{\kappa_{H\pm}}{m},
\end{aligned} \tag{18}$$

and $X_{1\pm} = m - n Y_{1\pm}$. The notations given in (18) will be used in figures for simulations and in bifurcation diagrams.

In the following analysis, P_1 denotes $P_{1\pm}$. It is easy to show that $\kappa_T > \kappa_{SN}$. Further, we treat κ as a bifurcation parameter, and the other two parameters e and n as control parameters. In addition, we call the Type-I bistable phenomenon (or Type-I coexistence of bistable states) if two stable equilibria coexist, and the Type-II bistable phenomenon (or Type-II coexistence of bistable states) if a stable equilibrium and a stable limit cycle coexist.

In [24], the following lemma about the stability and bifurcation of the equilibria P_0 and P_1 has been proved. However, whether the Hopf bifurcations are supercritical or subcritical is not proved in [24] since the conventional analytical method does not work

due to the complex expressions of y_{1-} and $\kappa_{H_{\pm}}$, which makes it impossible to compute the focus values or the normal forms associated with Hopf bifurcations. In the following, we first derive the explicit conditions on the parameters to classify the types of Hopf bifurcations, and then consider the codimension of Hopf bifurcations. For the readability of the readers, we list Theorem 2.1 in [24] for system (8) as a lemma below, with a modification to adapt system (11).

Lemma 2.1. *For the system (11), the infection-free equilibrium P_0 is asymptotically stable if the basic reduction number, $R_0 < 1$ (i.e., $\kappa < \kappa_T$), and unstable if $R_0 > 1$ (i.e., $\kappa > \kappa_T$). The infectious equilibrium P_1 does not exist for $\kappa < \kappa_{SN}$; P_{1-} exists only for $\kappa \geq \kappa_T$ and $e \leq e_1$; both $P_{1\pm}$ exist for $\kappa > \kappa_{SN}$ and $e > e_1$, with P_{1+} beign a saddle point. A transcritical bifurcation occurs between P_0 and P_1 at the critical point $\kappa = \kappa_T$. Hopf bifurcations can occur from the equilibrium P_{1-} under certain conditions on the parameters. More details are given below.*

- (I) *When $e \leq e_1$, no bistable phenomenon can happen. Moreover,*
- (I-a) *if $e \leq \min\{e_1, e_2\}$, then P_{1-} is asymptotically stable for $\kappa > \kappa_T$, and no Hopf bifurcation can happen;*
 - (I-b) *if $n \leq \frac{\sqrt{2}-1}{2}$ and $e_2 < e \leq e_1$, then two Hopf bifurcations occur at $\kappa = \kappa_{H-}$ and $\kappa = \kappa_{H+}$; P_{1-} is asymptotically stable for $\kappa \in (\kappa_T, \kappa_{H-}) \cup (\kappa_{H+}, \infty)$, and unstable for $\kappa \in (\kappa_{H-}, \kappa_{H+})$.*
- (II) *When $e > n + 1$, the following holds.*
- (II-a) *P_{1-} is asymptotically stable, and no Hopf bifurcation can happen if one of the following conditions is satisfied:*
 - (II-a-i) *$e \geq e_4$ and $\kappa > \max\{\kappa_{SN}, \kappa^*\}$;*
 - (II-a-ii) *$n < 1$, $e > \max\{e_3, e_4\}$ and $\kappa = \kappa^*$;*
 - (II-a-iii) *$n \geq \frac{\sqrt{2}-1}{2}$, $e_1 < e < \min\{e_2, e_4\}$ and $\kappa > \kappa_{SN}$ ($> \kappa^*$).**Type-I bistable phenomenon can occur in all the above three subcases.*
 - (II-b) *If $0 < n < \frac{1}{2}$, $e_3 < e \leq e_4$ and $\kappa_{SN} < \kappa \leq \kappa^*$, then P_{1-} is unstable, excluding Hopf bifurcation.*
 - (II-c) *One Hopf bifurcation occurs in the following cases.*

- (II-c-i) If $n < \frac{1}{2}$, $e_3 < e < e_4$ and $\kappa > \kappa^*$ ($> \kappa_{\text{SN}}$), then a Hopf bifurcation occurs at $\kappa = \kappa_{\text{H}_+}$; P_{1-} is asymptotically stable for $\kappa \in (\kappa_{\text{H}_+}, \infty)$, and unstable for $\kappa \in (\kappa_{\text{SN}}, \kappa_{\text{H}_+})$. Both type-I bistable states and Type-II bistable states coexist if $\frac{1}{3} \leq n < \frac{1}{2}$, or if $n < \frac{1}{3}$ with $e > e_+$, for which $\kappa_{\text{H}_+} < \kappa_{\text{T}}$.
- (II-c-ii) If $n < 1$, $e > \max\{e_3, e_4\}$ and $\kappa_{\text{SN}} < \kappa < \kappa^*$, then a Hopf bifurcation occurs at $\kappa = \kappa_{\text{H}_+}$; P_{1-} is asymptotically stable for $\kappa > \kappa_{\text{H}_+}$, and unstable for $\kappa \in (\kappa_{\text{SN}}, \kappa_{\text{H}_+})$. Both Type-I and Type-II bistable states coexist, since $\kappa_{\text{H}_+} < \kappa_{\text{T}}$.
- (II-d) Two Hopf bifurcations occur at $\kappa = \kappa_{\text{H}_-}$ and $\kappa = \kappa_{\text{H}_+}$ if $n < \frac{1}{2}$, $\max\{e_1, e_2\} < e < e_3$ and $\kappa \geq \kappa_{\text{SN}}$ ($> \kappa^*$); P_{1-} is asymptotically stable for $\kappa \in (\kappa_{\text{SN}}, \kappa_{\text{H}_-}) \cup (\kappa_{\text{H}_+}, \infty)$, and unstable for $\kappa \in (\kappa_{\text{H}_-}, \kappa_{\text{H}_+})$. Type-I bistable states coexist, and Type-II bistable states coexist if $\frac{\sqrt{5}-1}{4} \leq n < \frac{1}{2}$ and $e_2 < e < e_3$, or $n < \frac{\sqrt{5}-1}{4}$ and $e_- < e < e_3$ for which $\kappa_{\text{H}_-} < \kappa_{\text{T}}$; and if $\frac{\sqrt{5}-1}{4} \leq n < \frac{1}{3}$ and $e_2 < e < e_-$, or $\frac{1}{3} \leq n < \frac{1}{2}$ and $e_2 < e < e_3$ for which $\kappa_{\text{H}_+} < \kappa_{\text{T}}$.

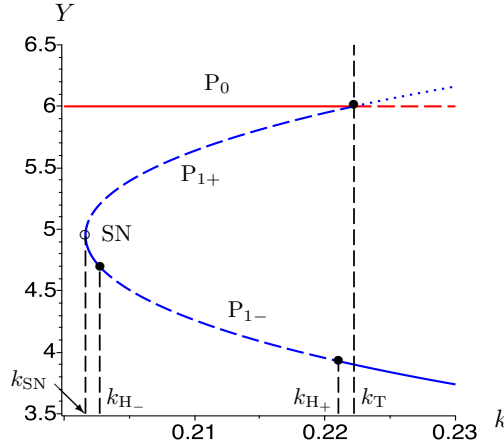


Figure 1: Bifurcation diagram for the model (8) projected on the k - Y plane with $m = 2$, $n = \frac{1}{3}$ and $\varepsilon = \frac{5}{4}$, corresponding to the Case (II-d) in Lemma 2.1 with $\kappa^* = \frac{640}{3243}$, $\kappa_{\text{SN}} = \frac{320}{1587}$ and $\kappa_{\text{SN}} = \frac{320}{1587}$, having two Hopf critical points at $\kappa_{\text{H}_\pm} = \frac{4035 \pm 17\sqrt{105}}{19044}$. The colored solid and dashed curves denote stable and unstable equilibria, respectively, while the dotted curve represents a mathematical solution without biological meaning.

The bifurcation diagram for the Case (II-d) is given in Figure 1 for system (8), with the parameter values: $m = 2$, $n = \frac{1}{3}$ and $\varepsilon = \frac{5}{4}$. Note that the notations given in (18) are used in the bifurcation diagrams. First note that P_1 , determined from $g = 0$, only

exists for $k \geq k_{\text{SN}}$. However, the part of the solution Y_1 satisfying $Y_1 > Y_{1\text{T}}$ is biologically meaningless since $X_1 < 0$ when $Y_1 > Y_{1\text{T}}$. On the bifurcation diagram, projected on the k - Y plane, $Y_1 = Y_{1*}$ and $Y_1 = Y_1^*$ are two horizontal asymptotes of the curve $g=0$ (which are not shown in the diagram), serving as the lower and upper boundaries of the solution P_1 . The curve has a unique vertex at $(k_{\text{SN}}, Y_{1\text{SN}})$. Moreover, using the derivative $\frac{dk}{dY_1}$, we can show that the solution Y_1 , determined by a function $k = k(Y_1)$, is monotonically decreasing for $Y_1 < Y_{1\text{SN}}$ and monotonically increasing for $Y_1 > Y_{1\text{SN}}$, like a parabola. Hence, when $Y_{1\text{SN}} \geq Y_{1\text{T}}$, i.e., when $\varepsilon \leq \varepsilon_1$, P_1 has one solution P_{1-} ; while when $Y_{1\text{SN}} < Y_{1\text{T}}$, i.e., when $\varepsilon > \varepsilon_1$, P_1 has two solutions: P_{1+} and P_{1-} , and P_{1+} exists for $Y_{1\text{SN}} \leq Y_1 \leq Y_{1\text{T}}$, while P_{1-} exists for $Y_{1*} < Y_1 \leq Y_{1\text{SN}}$. It is shown in the figure that there exist two Hopf bifurcations, and both Type-I and Type-II bistable phenomena exist because the chosen parameter values satisfy $k_{\text{SN}} < k_{\text{H-}} < k_{\text{H+}} < k_{\text{T}}$. Hence, two stable equilibria P_0 and P_{1-} coexist for $k \in (k_{\text{SN}}, k_{\text{H-}}) \cup (k_{\text{H+}}, k_{\text{T}})$, while stable P_0 and a stable limit cycle (which is verified by simulation and needs a rigorous proof) coexist for $k \in (k_{\text{H-}}, k_{\text{H+}})$.

Whether the Hopf bifurcations for the cases (I-b), (II-c) and (II-d) in Lemma 2.1 are supercritical or subcritical depends on the sign of the first-order focus value associated with the Hopf bifurcation. However, if one uses the expressions of the solution y_{1-} and the critical points $\kappa_{\text{H}\pm}$ given in (17) to derive the first-order focus value, it is impossible to compute the first-order focus value since the resulting equations are too complex to deal with. We will use a parameter which is linear in the function g , instead of y_1 , to solve $g = 0$. y_1 is then treated as a ‘‘parameter’’ in the stability and bifurcation analysis, because it is a component of the equilibrium solution P_1 and is indeed a function of the system parameters. Consequently, the stability conditions on the parameters need to be rederived using y_1 and the other parameters.

We have following result for determining whether the Hopf bifurcations in Lemma 2.1 are supercritical or subcritical.

Theorem 2.2. *Hopf bifurcation of system (11) exists for $0 < n < 1$, and it is supercritical for $0 < n \leq \frac{1}{3}$, and subcritical for $\frac{1}{2} \leq n < 1$. When $\frac{1}{3} < n < \frac{1}{2}$, Hopf bifurcation is supercritical if $e < e^*$, and subcritical if $e > e^*$, where*

$$e^* = \frac{n(n+1)^2}{(1-2n)\sqrt{(1+n)(1-2n)} + (n^2+2n-1)}, \quad n \in \left(\frac{1}{3}, \frac{1}{2}\right). \quad (19)$$

For the cases in Lemma 2.1, the Hopf bifurcations in the Cases (I-b), (II-c-i) and (II-d) are supercritical. For the Case (II-c-ii), the Hopf bifurcation is supercritical when $0 < n \leq \frac{1}{3}$, or when $\frac{1}{3} < n < \frac{1}{2}$ and $\max\{e_3, e_4\} < e < e^$; and subcritical when $\frac{1}{2} \leq n < 1$, or when $\frac{1}{3} < n < \frac{1}{2}$ and $e > e^*$.*

The proof of Theorem 2.2 is included in the proof for Theorem 2.3.

2.2. Codimension of Hopf bifurcation

In this section, we consider the codimension of the Hopf bifurcation from the positive equilibrium P_{1-} . Numerical examples have been given in [14] to show that both stable and unstable limit cycles can bifurcate from Hopf critical points. This implies that the first focus value may become zero, and thus at least 2 limit cycles can bifurcate due to the generalized Hopf bifurcation, leading to a codimension-2 Hopf bifurcation. We have the following theorem.

Theorem 2.3. *The system (11) has generalized Hopf bifurcation with codimension 2, yielding maximal 2 limit cycles enclosing an unstable equilibrium P_{1-} , and the inner limit cycle is stable while the outer one is unstable.*

Proof. [for Theorems 2.2 and 2.3] In order to derive the stability of P_1 for studying the codimension of Hopf bifurcation, we solve $g = 0$ for e , instead of y_1 , to obtain

$$e = \frac{y_{1*} + \frac{1}{\kappa} - y_1}{n(y_{1T} - y_1)(y_1 - y_{1*})}. \quad (20)$$

It follows from $e > 0$ that

$$y_{1*} < y_1 < \min \left\{ y_{1T}, y_{1*} + \frac{1}{\kappa} \right\}. \quad (21)$$

The stability of equilibria is determined from the Jacobian of system (11), given by

$$J(x, y) = \begin{bmatrix} \kappa [y - 2x + ex(2y - 3x)] - (n + 1) & \kappa x(1 + ex) \\ -1 & -n \end{bmatrix}.$$

Evaluating this Jacobian at $P_1 = (1 - ny_1, y_1)$ yields the trace and determinant of the Jacobian $J(P_1)$ as

$$\begin{aligned} \text{Tr}(J(P_1)) &= \frac{\kappa [(n + 1)y_1 - 1]^2 + n + 2 - (n + 1)^2 y_1}{(n + 1)y_1 - 1}, \\ \det(J(P_1)) &= \frac{(n + 1)^3 (ny_1 - 1)^2 + n(\kappa - \kappa_T) [(n + 1)y_1 - 1]^2}{(n + 1)y_1 - 1}. \end{aligned} \quad (22)$$

The determinant clearly shows that there exists a transcritical bifurcation between P_0 and P_1 at the critical point $\kappa = \kappa_T$ at which $\det(J(P_1)) = 0$ leads to $y_1 = \frac{1}{n}$.

Hopf bifurcation occurs when $\text{Tr}(J(P_1)) = 0$ and $\det(J(P_1)) > 0$. Note that the formulas given in (22) are applicable for both solutions y_{1+} and y_{1-} . In other words, the following results for P_1 include both $P_{1\pm}: (x_{1\pm}, y_{1\pm})$. However, we know from the results in the previous section that Hopf bifurcation can only occur from the equilibrium P_{1-} , since P_{1+} is a saddle point when it exists.

A necessary condition for system (11) to undergo a Hopf bifurcation is $\text{Tr}(J(P_1)) = 0$ which needs $(n+2) - (n+1)^2 y_1 < 0$, that is then combined with the condition (21) to yield

$$\frac{n+2}{(n+1)^2} < y_1 < \min \left\{ \frac{1}{n}, \frac{1}{n+1} + \frac{1}{\kappa} \right\} \quad \text{and} \quad \kappa < (n+1)^2. \quad (23)$$

Solving $\text{Tr}(J(P_1)) = 0$ for κ leads to the Hopf critical point, defined by

$$\kappa_H = \frac{(n+1)^2 y_1 - (n+2)}{[1 - (n+1)y_1]^2} = (n+1)^2 - \frac{[2(n+1)^2 y_1 - (2n+3)]^2 + 3}{4[1 - (n+1)y_1]^2}, \quad (24)$$

which indicates that $\kappa_H \in (0, (n+1)^2)$. Hence, the equilibrium P_1 is asymptotically stable if $\kappa \in (0, \kappa_H)$ (for which $\text{Tr}(J(P_1)) < 0$) and unstable if $\kappa \in (\kappa_H, (n+1)^2)$ (for which $\text{Tr}(J(P_1)) > 0$). Hopf bifurcation occurs from P_1 at the critical point $\kappa = \kappa_H$.

Next, in order to determine the stability of the bifurcating limit cycles, we need to compute the focus values. To achieve this, letting $\kappa = \kappa_H$ and introducing the following affine transformation,

$$\begin{pmatrix} x \\ y \end{pmatrix} = \begin{pmatrix} 1 - ny_1 \\ y_1 \end{pmatrix} + \begin{bmatrix} 1 & 0 \\ \frac{n[(n+1)y_1 - 1]}{(n+1)(ny_1 - 1)} & \frac{-\omega_c[(n+1)y_1 - 1]}{(n+1)(ny_1 - 1)} \end{bmatrix} \begin{pmatrix} u \\ v \end{pmatrix},$$

where

$$\omega_c = \sqrt{\frac{n^2 + n + 1 - n(n+1)^2 y_1}{(n+1)y_1 - 1}},$$

into (11) we obtain the following system,

$$\begin{aligned} \frac{du}{d\tau} &= \omega_c v - \frac{1}{(n+1)Q_1^2 Q_2^2} (Q_1 u^2 - \omega_c Q_1 Q_2 Q_3 uv + u^3 - \omega_c Q_2 u^2 v), \\ \frac{dv}{d\tau} &= -\omega_c u - \frac{n}{(n+1)Q_1^2 Q_2^2 \omega_c} (Q_1 u^2 - \omega_c Q_1 Q_2 Q_3 uv + u^3 - \omega_c Q_2 u^2 v), \end{aligned} \quad (25)$$

whose linear part is in the Jordan canonical form, where

$$Q_1 = 1 - ny_1, \quad Q_2 = (n+1)y_1 - 1, \quad Q_3 = (n+1)^2 y_1 - n.$$

Note that $\omega_c > 0$ requires that

$$y_1 < \frac{n^2 + n + 1}{n(n+1)^2} = \frac{1}{n} - \frac{1}{(n+1)^2}. \quad (26)$$

As a matter of fact, P_1 is a saddle point when $y_1 > \frac{1}{n} - \frac{1}{(n+1)^2}$, and a B-T bifurcation point when $y_1 = \frac{1}{n} - \frac{1}{(n+1)^2}$.

Combining the condition $y_1 > \frac{n+2}{(n+1)^2}$ in (23) and that in (26) yields that $\frac{n+2}{(n+1)^2} < \frac{1}{n} - \frac{1}{(n+1)^2}$, which in turn gives $n < 1$. Therefore, it follows from (23) and (26) that the restriction conditions on y_1 and κ are given by

$$y_{1L} < y_1 < y_{1U},$$

where

$$y_{1L} = \frac{n+2}{(n+1)^2}, \quad y_{1U} = \min \left\{ \frac{1}{n} - \frac{1}{(n+1)^2}, \frac{1}{n+1} + \frac{1}{\kappa_H} \right\}, \quad (0 < n < 1), \quad (27)$$

under which $Q_i > 0$, $i = 1, 2, 3$, and $n+1 - nQ_3 > 0$.

Now, applying the Maple program [19] for computing the normal form of Hopf and generalized Hopf bifurcations to system (25), we obtain the following focus values,

$$\begin{aligned} v_1 &= \frac{v_{1a}}{8(n+1)Q_1Q_2^3[n+1-nQ_3]}, \\ v_2 &= \frac{-v_{2a}}{192(n+1)^3Q_1^3Q_2^6[n+1-nQ_3]^3}, \\ v_3 &= \frac{v_{3a}}{18432(n+1)^5Q_1^5Q_2^9[n+1-nQ_3]^5}, \\ &\vdots \end{aligned} \quad (28)$$

showing that v_i and v_{ia} ($i = 1, 2, 3$) have the same sign. Here, v_{1a}, v_{2a}, \dots are polynomials

in n and y_1 . In particular,

$$\begin{aligned}
v_{1a} &= n(n+1)^4 y_1^2 - 2(n^2+n+1)(n+1)^2 y_1 + (n^3+2n^2+5n+3), \\
v_{2a} &= n^3(n+1)^{12}(28n+27)y_1^7 - n^2(n+1)^{10}(196n^3+350n^2+267n+108)y_1^6 \\
&\quad + n(n+1)^8(588n^5+1533n^4+2101n^3+1683n^2+672n+135)y_1^5 \\
&\quad - (n+1)^6(980n^7+3360n^6+6500n^5+7711n^4+5620n^3+2567n^2 \\
&\quad + 602n+54)y_1^4 + (n+1)^4(980n^8+4165n^7+10330n^6+16174n^5 \\
&\quad + 16730n^4+11680n^3+5215n^2+1400n+169)y_1^3 \\
&\quad - (n+1)^2(588n^9+2982n^8+8995n^7+17466n^6+23190n^5 \\
&\quad + 21409n^4+13397n^3+5563n^2+1443n+192)y_1^2 \\
&\quad + (n+1)(196n^9+959n^8+3138n^7+6349n^6+8961n^5+8410n^4 \\
&\quad + 4886n^3+1470n^2+84n-36)y_1 - 28n^9 - 132n^8 - 474n^7 \\
&\quad - 979n^6 - 1470n^5 - 1291n^4 - 460n^3 + 334n^2 + 517n + 189.
\end{aligned} \tag{29}$$

To find the maximal number of limit cycles bifurcating from the Hopf critical point, we need to find the solutions satisfying $v_k = 0$ as many as possible. Since there are only two free parameters (n, y_1) in v_k , the maximal number of bifurcating limit cycles can be three. However, in solving practical problems, due to the constraints on the parameters, this maximal number is usually not reachable. Now, let us first consider the possibility of 3 limit cycles. Eliminating y_1 from the two equations, $v_{1a} = v_{2a} = 0$, yields a solution for $y_1 = \bar{y}_1$, where

$$\bar{y}_1 = \frac{23 + (1-2n)[(1-2n)(1+14n+24n^2) + 46n^3]}{4(4+n) + 2n(1-2n)[(1-2n)(6+15n+28n^2) + 55n^3]}, \tag{30}$$

and a resultant equation:

$$\text{Res}(n) = n(2n+1)(3n^2-11n+11)(2n-1) = 0, \tag{31}$$

which has only one positive solution $n = \frac{1}{2}$ for which $\bar{y}_1 = \frac{23}{18}$, yielding $v_1 = \frac{3240}{17303} \neq 0$. Hence, bifurcation of 3 limit cycles is not possible, since it requires that $v_1 = v_2 = 0$.

The next best possibility is bifurcation of 2 limit cycles, which needs $v_1 = 0$. The discriminant of quadratic polynomial v_{1a} is

$$\Delta_1 = 4(1-2n)(n+1)^5.$$

Thus, $\Delta_1 < 0$ when $n > \frac{1}{2}$, yielding $v_{1a} > 0$ and so $v_1 > 0$. When $n = \frac{1}{2}$, the condition $\frac{n+2}{(n+1)^2} < y_1 < \frac{1}{n} - \frac{1}{(n+1)^2}$ is reduced to $\frac{10}{9} < y_1 < \frac{14}{9}$, and then v_1 becomes

$$v_1 = \frac{14 - 9y_1}{3m^2(2 - y_1)(3y_1 - 2)^3} > 0.$$

The above result indicates that when $\frac{1}{2} \leq n < 1$, the Hopf bifurcation is subcritical and bifurcating limit cycles are unstable. When $n < \frac{1}{2}$, solving the quadratic polynomial equation $v_{1a} = 0$ yields two real positive solutions,

$$y_{1\pm} = \frac{1}{n(n+1)^2} \left[n^2 + n + 1 \pm \sqrt{(1-2n)(n+1)} \right]. \quad (32)$$

Hence, $v_{1a} < 0$ for $y_1 \in (y_{1-}, y_{1+})$ and $v_{1a} > 0$ for $y_1 \in (0, y_{1-}) \cup (y_{1+}, \infty)$.

Moreover, it is easy to show that

$$y_{1-} < \frac{1}{n} - \frac{1}{(n+1)^2} < y_{1+},$$

and

$$y_{1-} \geq y_{1L} = \frac{n+2}{(n+1)^2} \iff \sqrt{(1-2n)(n+1)} \leq 1-n \iff n(3n-1) \geq 0.$$

Therefore, for $n \leq \frac{1}{3}$, the condition $y_{1-} \leq y_{1L}$ implies that any feasible values of y_1 for Hopf bifurcation satisfy

$$y_{1-} \leq y_{1L} < y_1 < y_{1U} \leq \frac{1}{n} - \frac{1}{(n+1)^2} < y_{1+},$$

and so $v_{1a} < 0$, that is, $v_1 < 0$. Hence, the Hopf bifurcation is supercritical and bifurcating limit cycles are stable for $0 < n \leq \frac{1}{3}$. Summarizing the above results, we have shown that one limit cycle can be generated from Hopf bifurcation for $n \in (0, \frac{1}{3}] \cup [\frac{1}{2}, 1)$, and the Hopf bifurcation is supercritical if $n \in (0, \frac{1}{3}]$, and subcritical if $n \in [\frac{1}{2}, 1)$. The conditions under which two limit cycles can occur from a Hopf bifurcation are given by

$$\frac{1}{3} < n < \frac{1}{2}, \quad y_1 = y_{1-} \implies v_1 = 0, \quad \text{and thus} \quad y_1 \geq y_{1-} \iff v_1 \leq 0.$$

Further, it can be shown by using (27) that for $\frac{1}{3} < n < \frac{1}{2}$, the following holds:

$$\begin{aligned} & \frac{1}{n} - \frac{1}{(n+1)^2} < \frac{1}{n+1} + \frac{1}{\kappa_H} \\ \iff & \frac{1}{n} - \frac{1}{(n+1)^2} - \frac{1}{n+1} - \frac{1}{\kappa_H} < 0 \\ \iff & -\frac{n(n+1)^4 y_1^2 - (2n^2 + 2n + 1)(n+1)^2 y_1 + n^3 + 2n^2 + 2n + 2}{n(n+1)^2[(n+1)^2 y_1 - (n+2)]} < 0, \end{aligned}$$

because the discriminant of the numerator of the left-hand side of the last inequality in the above is equal to $-(n+1)^4(4n-1) < 0$ for $n \in (\frac{1}{3}, \frac{1}{2})$. This implies that $y_{1U} = \frac{1}{n} - \frac{1}{(n+1)^2}$

and $y_{1L} < y_{1-} < y_{1U} < y_{1+}$ for $n \in (\frac{1}{3}, \frac{1}{2})$. Consequently, when $n \in (\frac{1}{3}, \frac{1}{2})$, the Hopf bifurcation is supercritical for $y_1 \in (y_{1-}, y_{1U})$ ($v_1 < 0$), and subcritical for $y_1 \in (y_{1L}, y_{1-})$ ($v_1 > 0$).

To transform the above stability expression in y_1 back to that in the parameter e , we substitute $\kappa = \kappa_H$ and y_1 into e in (20) to obtain

$$e(y_1) = \frac{1}{(1 - ny_1)[(n+1)^2 y_1 - (n+2)]} > 0, \quad \text{for } y_{1L} < y_1 < y_{1U}.$$

Then, substituting $y_1 = y_{1-}$ into $e(y_1)$ yields $e^* = e(y_{1-})$. Further, we can show that

$$\frac{de(y_1)}{dy_1} = \frac{2n(n+1)^2 y_1 - (2n^2 + 4n + 1)}{(1 - ny_1)^2 [(n+1)^2 y_1 - (n+2)]^2} \begin{cases} < 0, & \text{for } y_1 < y_{1\min}, \\ > 0, & \text{for } y_1 > y_{1\min}, \end{cases} \quad y_{1\min} = \frac{2n^2 + 4n + 1}{2n(n+1)^2}.$$

It is easy to prove that $y_{1L} < y_{1\min} < y_{1U}$, and $y_{1-} < y_{1\min}$.

In addition, a direct computation leads to that

$$e^* - e(y_{1U}) = e^* - e_3 = \frac{(1+n)^2(1-2n)[(1+n)(5n-2) - (1-n)\sqrt{(1+n)(1-2n)}]}{(1-n)(3n-1)(3n^2+n-1)} > 0$$

for $\frac{1}{3} < n < \frac{1}{2}$. This clearly indicates that $e < e^*$ (respectively $e > e^*$) when $y_1 > y_{1-}$ (respectively $y_1 < y_{1-}$). Hence, for $n \in (\frac{1}{3}, \frac{1}{2})$, the Hopf bifurcation is supercritical (respectively subcritical) if $e < e^*$ (respectively $e > e^*$). This finishes the proof for the first part of Theorem 2.2.

Now, based on the above established results, we consider the Hopf bifurcations in Lemma 2.1. For the Case (I-b), it is obvious that the two Hopf bifurcations are supercritical since $n \leq \frac{\sqrt{2}-1}{2} < \frac{1}{3}$, and bifurcating limit cycles are stable. For the Case (II-c)(i), with the condition $n < \frac{1}{2}$ and $e_3 < e < e_4$, we know that the Hopf bifurcation is supercritical for $0 < n \leq \frac{1}{3}$. When $\frac{1}{3} < n < \frac{1}{2}$, similar to prove $e_3 < e^*$, we can show that $e_4 < e^*$, which yields $e < e^*$. Thus, the Hopf bifurcation is also supercritical for $\frac{1}{3} < n < \frac{1}{2}$. For the Case (II-c-ii) with the condition $n < 1$ and $e > \max\{e_3, e_4\}$, the Hopf bifurcation is supercritical for $0 < n \leq \frac{1}{3}$, and subcritical for $\frac{1}{2} \leq n < 1$. When $\frac{1}{3} < n < \frac{1}{2}$, it has been shown in the above that $e > \max\{e_3, e_4\}$, the Hopf bifurcation is supercritical for $\max\{e_3, e_4\} < e < e^*$, and subcritical for $e > e^*$.

This finishes the proof for Theorem 2.2.

To prove Theorem 2.3, note that we have shown that $v_1 = 0$ at $y_1 = y_{1-}$ (or at $e = e^*$), indicating that two limit cycles can bifurcate from the Hopf critical point $\kappa = \kappa_H$ if $e = e^*$. To complete the proof for Theorem 2.3, we need to verify $v_2 \neq 0$ when $v_1 = 0$ (i.e., at

$y_1 = y_{1-}$ or $e = e^*$). Substituting the solutions y_{1-} into v_2 we obtain

$$v_2|_{v_1=0} = \frac{-\tilde{v}_2}{48n^3(1-2n)(n+1)^9[\sqrt{(1-2n)(n+1)}+n]^6[\sqrt{(1-2n)(n+1)}-1]^6},$$

where

$$\begin{aligned}\tilde{v}_2 &= [(1-2n)(8+8n+15n^2)+32n^3]\sqrt{(1-2n)(n+1)} \\ &\quad - [(1-2n)(8+4n+2n^2+11n^3)+20n^4],\end{aligned}$$

whose sign is the same as that of

$$\begin{aligned}\tilde{v}_2 &= [(1-2n)(8+8n+15n^2)+32n^3]^2(1-2n)(n+1) \\ &\quad - [(1-2n)(8+4n+2n^2+11n^3)+20n^4]^2 \\ &= -n^4(2n+1)^2(3n^2-11n+11) < 0,\end{aligned}$$

yielding $\tilde{v}_2 < 0$, that is, $v_2|_{v_1=0} > 0$. This shows that the codimension of the Hopf bifurcation is indeed two. Moreover, the outer bifurcating limit cycle is unstable and the inner one is stable, and both them enclose an unstable focus P_{1-} .

Finally, we want to show that the generalized Hopf bifurcation, leading to bifurcation of 2 limit cycles under the condition $\frac{1}{3} < n < \frac{1}{2}$, can only occur in Case (II-c-ii). First, it is easy to see that it is not possible for the Case (I-b) since it requires $n < \frac{\sqrt{2}-1}{2}$. Then, with the condition $\frac{1}{3} < n < \frac{1}{2}$, we can show that $e > e_3$ and $e > e_4$. By using (20) with $y_1 = y_{1-}$ given in (32) and $\kappa = \kappa_H$ given in (24), we obtain

$$e = \frac{(n+1)^2[1-n+\sqrt{(1-2n)(n+1)}]}{(3n-1)[n+\sqrt{(1-2n)(n+1)}]}.$$

Then, a direct computation shows that

$$\begin{aligned}e - e_3 &= \frac{(n+1)^2(1-2n)[1+n+2\sqrt{(1-2n)(n+1)}]}{(1-n)(3n-1)[n+\sqrt{(1-2n)(n+1)}]} > 0, \\ e - e_4 &= \frac{(n+1)^2(1-2n)[2n+\sqrt{(1-2n)(n+1)}]}{n(3n-1)[n+\sqrt{(1-2n)(n+1)}]} > 0,\end{aligned}$$

for $\frac{1}{3} < n < \frac{1}{2}$. This indicates that 2 limit cycles cannot occur in Cases (II-c-i) and (II-d), and can only bifurcate in Case (II-c-ii), for which $\varepsilon > \max\{\varepsilon_3, \varepsilon_4\}$, and it can be shown that $\kappa_{SN} < \kappa_{H+} < \kappa^*$ as follows:

$$\begin{aligned}\kappa_{H+} - \kappa_{SN} &= \frac{2en(1-n^2)^2(e-e_3)^2}{(e+e_1)^2\{e[n(e+e_4)-e_2]+n(e-e_4)\sqrt{e(e-e_2)}\}} > 0, \\ \kappa^* - \kappa_{H+} &= \frac{2en(1+n)(1-n^2)^2(e-e_3)(e-e_4)}{(e+e_1)^2\{e(e-e_4)+n(e-e_4)\sqrt{e(e-e_2)}\}} > 0,\end{aligned}$$

since for this case, we have $e > e_4 > e_3 > e_2 > e_1$, and

$$n(e + e_4) - e_2 > 2ne_4 - e_2 = 2(1 - 2n)(n + 1)^2 > 0.$$

The proof for Theorem 2.3 is complete. \square

2.3. Simulations

Simulations for the stable limit cycles in the Cases (I-b), (II-c-i) and (II-d), as well as an unstable limit cycle in the Case (II-c-ii) with $n = \frac{3}{4} \in [\frac{1}{2}, 1)$ have been shown in [24]. In [14], the authors used system (8) to give four simulations to show the existence of bifurcating limit cycles, among them three are stable, and one is unstable. The parameter values for these simulations are given below, with our formula v_1 in (28) and (29) to confirm the stability (with the bold-faced numbers for the values of n). In order to keep consistent with the results given in [14], we also use (8) for our simulation, which will give the same results obtained by using (11) under the transformation (10).

$$\begin{aligned} \text{Stable LC : } (m, n, \varepsilon, k) &= (1.6, \mathbf{0.30}, 1.50, 0.25), & v_1 &= -0.082227, \\ &= (2.0, \mathbf{0.25}, 1.50, 0.15625), & v_1 &= -0.038194, \\ &= (1.5, \mathbf{0.30}, 1.55, 0.25), & v_1 &= -0.135503, \end{aligned}$$

$$\text{Unstable LC : } (m, n, \varepsilon, k) = (11.07825, \mathbf{0.4771}, 0.995, 0.0295), \quad v_1 = +0.001773.$$

It is not surprising to see that the first three values of n are less than $\frac{1}{3}$, yielding stable limit cycles. For the last example, $n = 0.4771 \in (\frac{1}{3}, \frac{1}{2})$, and using the formula (19), we obtain $\varepsilon^* = 0.485004 < \varepsilon = 0.995$, yielding $v_1 = 0.001773$ and thus the Hopf bifurcation is subcritical and the bifurcating limit cycle is unstable, as shown in Figure 2(a). However, for this case when $n \in (\frac{1}{3}, \frac{1}{2})$, the Hopf bifurcation is not necessarily subcritical. Parameters can be changed to get a supercritical Hopf bifurcation. For example, keeping $n = 0.4771$ unchanged and the following values for other parameter values, we obtain

$$\text{Stable LC : } (m, n, \varepsilon, k) = (10.5, \mathbf{0.4771}, 0.43, 0.0509),$$

which yields $\varepsilon^* = 0.511714 > \varepsilon = 0.43$ and $v_1 = -0.000831$, implying that the Hopf bifurcation is supercritical and the bifurcating limit cycle is stable, see Figure 2(b). It can be seen that the limit cycles shown in Figures 2(a) and 2(b) are pretty large and so the Hopf bifurcation prediction for the amplitude based on the normal forms might be not applicable. The Hopf critical value for Figures 2(a) and 2(b) are $k_H \approx 0.029221$ and $k_H \approx 0.050942$, respectively, which yields the perturbations $\mu \approx 0.000279$ ($\frac{\mu}{k_H} = 0.96\%$)

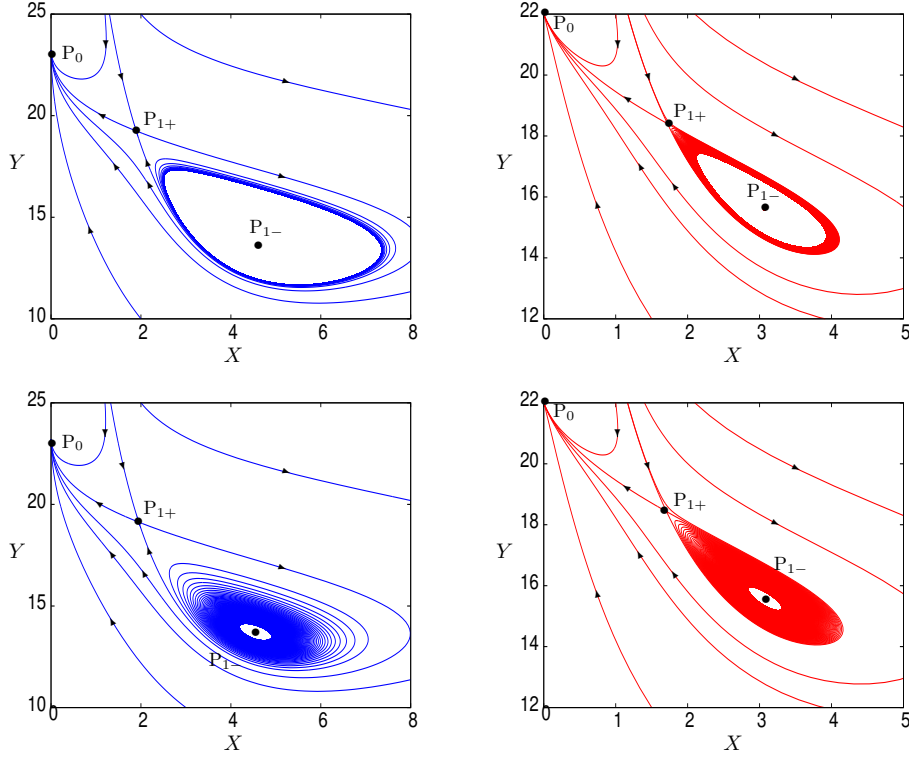


Figure 2: Simulated phase portraits for the Case (II-c-ii) of the model (8) with $n = 0.4771$: (a) an unstable limit cycle for $m=11.07825$, $\varepsilon=0.995$ and $k=0.0295$ [14]; (b) a stable limit cycle for $m=10.5$, $\varepsilon=0.43$ and $k=0.0509$; (c) an unstable limit cycle for $m=11.07825$, $\varepsilon=0.995$ and $k=0.029225$; and (d) a stable limit cycle for $m=10.5$, $\varepsilon=0.43$ and $k=0.05094$.

and $\mu \approx 0.000042$ ($\frac{\mu}{k_H} = 0.08\%$) for Figures 2(a) and 2(b), respectively. This indicates that the perturbations for both cases are actually small, but they yield the approximation for the amplitudes of the two small limit cycles as $r = 2.4734$ and $r = 0.8514$, respectively. They are pretty large, but it is interesting that the normal forms still predict their correct stability. For a comparison, we present another two simulations depicted in Figures 2(c) and 2(d), corresponding to $k = 0.029225$ (giving $\mu \approx 0.000004$ and $\frac{\mu}{k_H} = 0.015\%$) and $k = 0.05094$ (giving $\mu \approx 0.000002$ and $\frac{\mu}{k_H} = 0.005\%$), respectively. Both bifurcating limit cycles are quite small, with unstable and stable ones for the former and latter cases, respectively. The normal forms for these two cases predict the amplitudes for the two limit cycles as $r \approx 0.3142$ and $r \approx 0.2055$, respectively, showing that Hopf bifurcation theory is perfectly applicable.

For the two limit cycles arising from Hopf bifurcation, there exists an infinite set of

parameter values. For example, we first choose $m = 2$ since it is free, and then take

$$n = \frac{5}{11} \in \left(\frac{1}{3}, \frac{1}{2}\right),$$

yielding the values for the critical point,

$$y_1 = y_{1-} = \frac{Y_{1-}}{2} = \frac{1727}{1280}, \quad k_H = \frac{1280}{5929}, \quad \varepsilon^* = \frac{320}{99},$$

for which $v_0 = v_1 = 0$, $v_2 = \frac{46661632000}{845676707337}$. It is easy to verify that the above parameter values belong to the case (II-c-ii) in Lemma 2.1. Only one Hopf critical point exists in this case.

Then, perturbing y_1 and k as follows:

$$y_1 = y_{1-} + \varepsilon_1, \quad k = k_H + \varepsilon_2, \quad \text{where } \varepsilon_1 = \frac{1}{100}, \quad \varepsilon_2 = -\frac{1}{50000},$$

we obtain

$$k = \frac{203821518599}{924070050000} \quad \text{and} \quad \varepsilon = \frac{3407490109063040}{1096763591581219}.$$

For these perturbed parameter values, we have the normal form for the amplitude of oscillation up to 5th-order, given by

$$\begin{aligned} \dot{r} &= r \left(v_0 + v_1 r^2 + v_2 r^4 \right) \\ &= r \left(\frac{4299}{2200000000} - \frac{216980684800000}{83938145042658897} r^2 + \frac{14817759528898477514254458827898880000000}{200973840260810036901676626005378422866729} r^4 \right). \end{aligned}$$

Setting $\dot{r} = 0$ gives the approximate solutions for the amplitudes of the two limit cycles:

$$r_1 \approx 0.105015, \quad r_2 \approx 0.155024.$$

The simulation of this numerical example is shown in Figure 3. It is seen from this figure that the amplitudes of the simulated two limit cycles agree very well with the analytical predictions given above.

3. B-T bifurcation of system (11)

In this section, we present an analysis on the B-T bifurcation of system (11). In [14], the classical method was used to find the condition for codimension-2 B-T bifurcation for system (8). In [13], the six-step transformation approach was applied to analyze the codimension-3 B-T bifurcation of system (8).

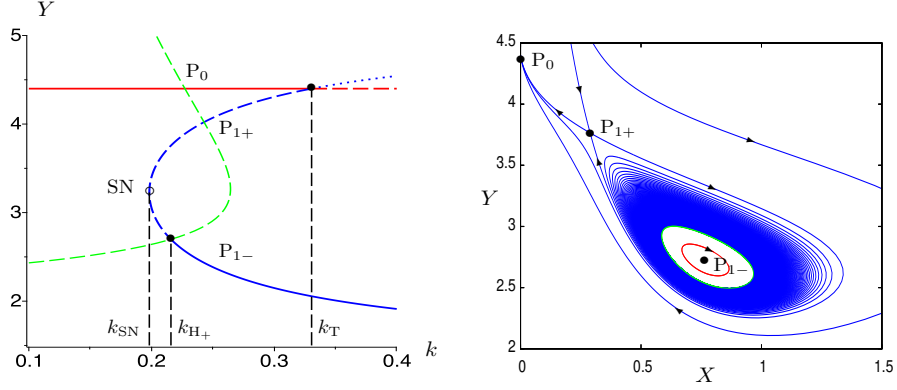


Figure 3: (a) Bifurcation diagram for the epidemic model (8) projected on the k - y_1 plane for $m = 2$, $n = \frac{5}{11}$ and $\varepsilon = \frac{320}{99}$, corresponding to the Case (II-c-ii) in Lemma 2.1 having one Hopf critical point, with $k_{SN} = \frac{57600}{290521}$, $k_{H+} = \frac{1280}{5929}$ and $k_T = \frac{40}{121}$; and (b) simulation of 2 limit cycles for perturbed values $k = \frac{203821518599}{924070050000}$ and $\varepsilon = \frac{3407490109063040}{1096763591581219}$, with the outer one unstable (in green color) and inner one stable (in red color).

3.1. Determining the codimension of B-T bifurcation

Here, we apply the SNF theory [20–22] to determine the codimension of B-T bifurcation. To achieve this, we first use κ to solve the equation $g = 0$, where the function g is given in (14), and then use y_1 and e to solve $\text{Tr}(J(P_1)) = \det(J(P_1)) = 0$ to obtain

$$\kappa = n(1-n)(1+n)^2, \quad e = \frac{(1+n)^2}{1-n}, \quad x_1 = \frac{n}{(1+n)^2}, \quad y_1 = \frac{n^2+n+1}{n(1+n)^2}, \quad (33)$$

which requires $0 < n < 1$. Then, introducing the affine transformation,

$$\begin{pmatrix} x \\ y \end{pmatrix} = \begin{pmatrix} \frac{n}{(1+n)^2} \\ \frac{n^2+n+1}{n(1+n)^2} \end{pmatrix} + \begin{bmatrix} n & 1 \\ -1 & 0 \end{bmatrix} \begin{pmatrix} u \\ v \end{pmatrix} \quad (34)$$

into (11) yields

$$\begin{aligned} \frac{du}{d\tau} &= v, \\ \frac{dv}{d\tau} &= -(n+1)^3(nu+v)[n^2u+(n-1)v] - n(n+1)^4(nu+v)^2[(n+1)u+v]. \end{aligned} \quad (35)$$

Next, applying the 5th-order change of variables:

$$\begin{aligned}
u &= y_1 - \frac{(n+1)^2(2n^2-1)}{4} y_1^2 - \frac{(n+1)(n^2+n+1)(2n^2-3n-1)(2n^2+4n+1)}{12n^2} y_1 y_2 \\
&\quad - \frac{(n+1)(20n^5-80n^3+16n^2+5n+4)}{240n^4} y_2^2 + \dots \\
v &= y_2 - (n-1)(n+1)^3 y_1 y_2 - \frac{(n+1)(2n^2-3n-1)(2n^2+4n+1)}{12n^2} y_2^2 + \dots
\end{aligned}$$

and the time scaling,

$$\tau = \left[1 + \frac{(n+1)^2}{2m} y_1 + t_{30} y_1^3 \right] \tau_1,$$

where t_{30} is a function in n , into (11) yields the SNF up to 5-th order as follows:

$$\begin{aligned}
\frac{dy_1}{d\tau_1} &= y_2, \\
\frac{dy_2}{d\tau_1} &= c_{20} y_1^2 + c_{11} y_1 y_2 + c_{31} y_1^3 y_2 + c_{41} y_1^4 y_2,
\end{aligned} \tag{36}$$

in which

$$\begin{aligned}
c_{20} &= -n^3(n+1)^3, \\
c_{11} &= -n(n+1)^3(2n-1), \\
c_{31} &= -\frac{(n+1)^6(40n^5+44n^4-18n^3+9n^2-7n+2)}{40}, \\
c_{41} &= \dots,
\end{aligned}$$

which shows that $c_{20} < 0$, and $c_{11} \neq 0$ if $n \neq \frac{1}{2}$. It should be pointed out that since we know $c_{20} \neq 0$ from the computation, we can assume the SNF in the form given in (36). This implies that higher codimension B-T bifurcation can only occur when $c_{11} = 0$, leading to the so-called degenerate cusp B-T bifurcation. If c_{20} can be zero, then we need to consider a different form of the SNF for the case $c_{20} = 0$.

When $n = n_0 = \frac{1}{2}$, we have

$$\kappa_0 = \frac{9}{16}, \quad e_0 = \frac{9}{2}, \quad x_1^0 = \frac{2}{9}, \quad y_1^0 = \frac{14}{9}, \tag{37}$$

and

$$c_{20} = -\frac{27}{64}, \quad c_{11} = 0, \quad c_{31} = -\frac{729}{1024} \neq 0.$$

Therefore, we have the following result.

Theorem 3.1. *For system (11), B-T bifurcation occurs from the endemic equilibrium P_1 : $(\frac{n}{(n+1)^2}, \frac{n^2+n+1}{n(n+1)^2})$ at the critical point $(e, \kappa) = (\frac{(n+1)^2}{1-n}, n(1-n)(n+1)^2)$, with $0 < n < 1$. Moreover, the B-T bifurcation is*

- (i) codimension 2 if $n \in (0, \frac{1}{2}) \cup (\frac{1}{2}, 1)$; or
- (ii) codimension 3 if $n = \frac{1}{2}$.

3.2. Codimension-2 B-T bifurcation

In [14], with m involved in the parameter set, a number of transformations were applied to obtain the normal form with unfolding up to second order. In the following, we apply our one-step transformation approach to derive the parametric simplest normal form (PSNF) [5–7, 22]. Let

$$\kappa = n(1-n)(n+1)^2 + \mu_1, \quad e = \frac{(n+1)^2}{1-n} + \mu_2, \quad (38)$$

which, together with the transformation (34), is substituted into (11) to yield the following system up to second-order terms,

$$\begin{aligned} \frac{du}{d\tau} &= v, \\ \frac{dv}{d\tau} &= \frac{1}{(1+n)^3(1-n)} \mu_1 + \frac{n^2(1-n)}{(1+n)^3} \mu_2 + \sum_{i+j+k+l=2} p_{ijkl} u^i v^j \mu_1^k \mu_2^l, \end{aligned} \quad (39)$$

where p_{ijkl} 's are coefficients expressed in terms of the parameter n . Next, applying the change of variables,

$$\begin{aligned} u &= -\frac{1}{n^3(1+n)^3} y_1 - \frac{1}{2n^4(1+n)^4} \beta_1 + \frac{1}{n(1+n)^3} \beta_2 - \frac{n^2-2}{4n^7(n+1)^5} \beta_1 y_1 \\ &\quad - \frac{2n^2-n+1}{n^4(1+n)^4(1-n)} \beta_2 y_1 + \frac{1-n}{2n^6(1+n)^3} y_1^2 - \frac{2n^3+n^2-5n-2}{6n^7(1+n)^5} y_1 y_2, \\ v &= -\frac{1}{n^3(1+n)^3} y_2 - \frac{2n^3+n^2-5n-2}{6n^7(1+n)^5} \beta_1 y_1 - \frac{n^2-2}{4n^7(1+n)^5} \beta_1 y_2 \\ &\quad + \frac{2n^2-n+1}{n^4(1+n)^4(1-n)} \beta_2 y_2 + \frac{1-n}{n^6(1+n)^3} y_1 y_2 - \frac{2n^3+n^2-5n-2}{6n^7(1+n)^5} y_2^2, \end{aligned} \quad (40)$$

and the parametrization,

$$\begin{aligned} \mu_1 &= -\frac{1-n}{n^3} \beta_1 - 2n^2(1+n) \beta_2, \\ \mu_2 &= \frac{2(1+n)}{(1-n)^2} \beta_2 + \frac{(1+n)(3n-1)}{n(1-n)^3} \beta_2^2, \end{aligned} \quad (41)$$

into (39), we obtain the PSNF up to second-order terms:

$$\begin{aligned} \frac{dy_1}{d\tau} &= y_2, \\ \frac{dy_2}{d\tau} &= \beta_1 + \beta_2 y_2 + y_1^2 - \frac{1-2n}{n^2} y_1 y_2, \quad \text{for } n \in \left(0, \frac{1}{2}\right) \cup \left(\frac{1}{2}, 1\right). \end{aligned} \quad (42)$$

Note from the above equation that the coefficient of $y_1 y_2$ is not normalized into ± 1 in order to show the direct effect of the original system parameter n on the dynamics of the system. It is clear that this coefficient can be positive or negative. Also, note that there is a negative multiplier $-\frac{1}{n^3(n+1)^3}$ in the transformation from (u, v) to (y_1, y_2) .

Based on the PSNF (42), we have the following bifurcation result.

Theorem 3.2. *For the system (11), codimension-2 B-T bifurcation occurs from the equilibrium $P_1 : (x, y) = (\frac{n}{(n+1)^2}, \frac{n^2+n+1}{n(n+1)^2})$ when $\kappa = n(1-n)(n+1)^2$ and $e = \frac{(n+1)^2}{1-n}$ if $n \in (0, \frac{1}{2}) \cup (\frac{1}{2}, 1)$. Moreover, three local bifurcations with the representations of the bifurcation curves are given below.*

(1) *Saddle-node bifurcation occurs from the bifurcation curve:*

$$\text{SN} = \left\{ (\beta_1, \beta_2) \mid \beta_1 = 0, \begin{cases} \beta_2 < 0 & (0 < n < \frac{1}{2}) \\ \beta_2 > 0 & (\frac{1}{2} < n < 1) \end{cases} \right\}.$$

(2) *Hopf bifurcation occurs from the bifurcation curve:*

$$\text{H} = \left\{ (\beta_1, \beta_2) \mid \beta_1 = -\frac{n^4}{(1-2n)^2} \beta_2, \begin{cases} \beta_2 < 0 & (0 < n < \frac{1}{2}), \text{ supercritical} \\ \beta_2 > 0 & (\frac{1}{2} < n < 1), \text{ subcritical} \end{cases} \right\}.$$

(3) *Homoclinic loop bifurcation occurs from the bifurcation curve:*

$$\text{HL} = \left\{ (\beta_1, \beta_2) \mid \beta_1 = -\frac{49}{25} \frac{n^4}{(1-2n)^2} \beta_2, \begin{cases} \beta_2 < 0 & (0 < n < \frac{1}{2}), \text{ stable} \\ \beta_2 > 0 & (\frac{1}{2} < n < 1), \text{ unstable} \end{cases} \right\}.$$

The above formulas for bifurcation curves can be expressed in terms of the original perturbation parameters μ_1 and μ_2 by using (40). The bifurcation diagram is depicted in Figure 4.

In the following, we present simulations for the codimension-2 B-T bifurcations discussed above to illustrate the theoretical results. In order to give a direct impression of the original system's dynamical behaviours, we use the model (8), rather than the normal forms (42) to perform the simulations. We choose $m = 2$, and two values of n : $n = \frac{2}{5} \in (0, \frac{1}{2})$, and $n = \frac{3}{4} \in (\frac{1}{2}, 1)$. For $n = \frac{2}{5}$, using the formulas given in (38)-(41), we transform the bifurcation diagram in Figure 4(a) back to that for the original model (8) near the B-T critical point plotted in the k - ε plane, as shown in Figure 5(a). On the other hand, a bifurcation diagram directly based on the model (8) is given in Figure 5(b). It is seen that the bifurcation diagram based on the normal form (42) (see Figure 4(a)) gives

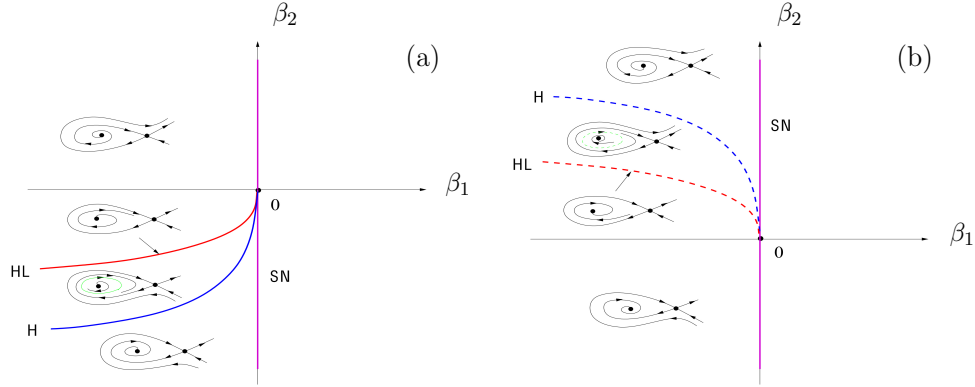


Figure 4: Bifurcation diagrams for the codimension-2 B-T bifurcation of the model (8) based on the normal form (42): (a) for $0 < n < \frac{1}{2}$; and (b) for $\frac{1}{2} < n < 1$.

a good indication for the dynamical behaviour of the original model near the B-T critical point. Moreover, the vertical line $\beta_1 = 0.01$ in the bifurcation diagram in Figure 4(a) is mapped to a curve (almost a straight line) in Figure 5(a). Therefore, we use the direct bifurcation diagram in Figure 5(b) and choose four points on the straight line (in green color),

$$11\varepsilon + 300k = 90, \quad \text{with } \varepsilon = 1.55, 1.60, 1.676171875, 1.80.$$

The corresponding simulated phase portraits are shown in Figure 6(a), (b), (c) and (d), respectively, representing the stable focus P_{1-} , a stable limit cycle and the unstable P_{1-} , the stable homoclinic loop, and the unstable P_{1-} . These phase portraits exactly correspond to that in Figure 4(a) in the upward direction.

Next, consider $n = \frac{3}{4}$. The bifurcation diagram is given in Figure 7(a). The region between the saddle-node bifurcation curve and the Hopf bifurcation curve is quite narrow, and a zoomed region is shown in Figure 7(b). Again, we choose four points from the line,

$$\varepsilon = 8, \quad \text{with } k = 0.2336, 0.23395, 0.23426542, 0.2345,$$

and the corresponding simulated phase portraits are depicted in Figure 8(a), (b), (c) and (d), respectively, representing the unstable focus P_{1-} , an unstable limit cycle and the stable P_{1-} , the unstable homoclinic loop, and the stable P_{1-} . These phase portraits exactly correspond to those in Figure 4(b) in the downward direction.

3.3. Codimension-3 B-T bifurcation

In this section, we consider codimension-3 B-T bifurcation for the epidemic model (8). First, we give a brief summary on the six-step transformation approach, and then

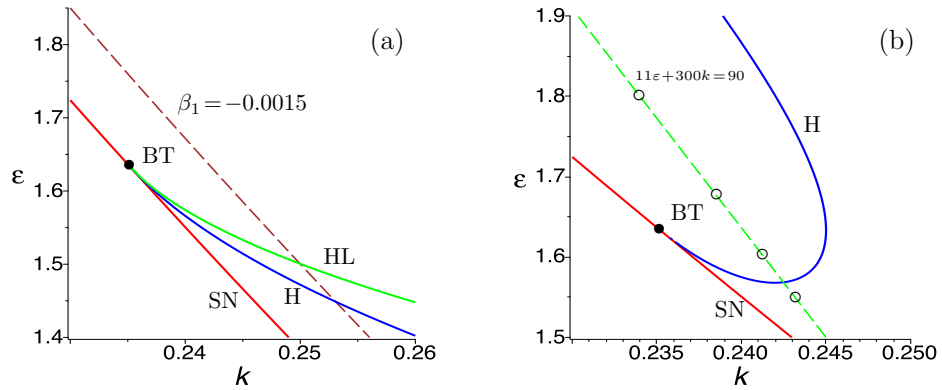


Figure 5: Bifurcation diagrams for the codimension-2 B-T bifurcation of the model (8) with $m=2$ and $n=\frac{2}{5}$: (a) based on the PSNF (42), where the straight line (in brown color) corresponds to the vertical line $\beta_1 = -0.0015$ in the bifurcation diagram in Figure 4(a); and (b) based on the model (8), with four points chosen from the line $11\varepsilon+300k=90$, with $\varepsilon=1.55, 1.60, 1.676171875$ and 1.80 , respectively.

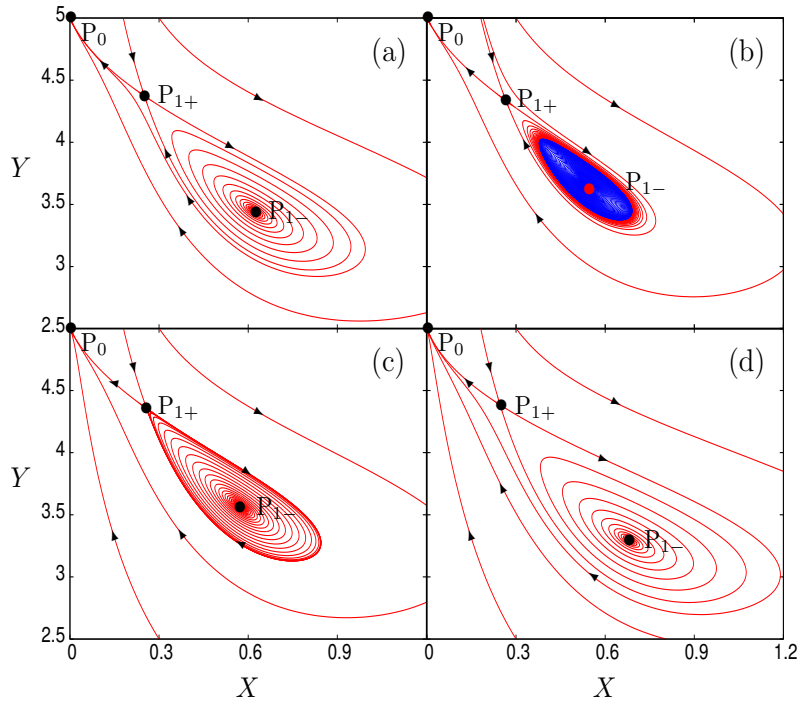


Figure 6: Simulated phase portraits for the codimension-2 B-T bifurcation of the epidemic model (8) with $m=2$, $n=\frac{2}{5}$, and $k = \frac{90-11\varepsilon}{300}$, for (a) $\varepsilon = 1.55$ showing the stable focus P_{1-} , (b) $\varepsilon = 1.60$ showing Hopf bifurcation yielding a stable limit cycle and the unstable P_{1-} , (c) $\varepsilon = 1.676171875$ showing the stable homoclinic loop and unstable P_{1-} , and (d) $\varepsilon = 1.80$ showing the unstable focus P_{1-} .

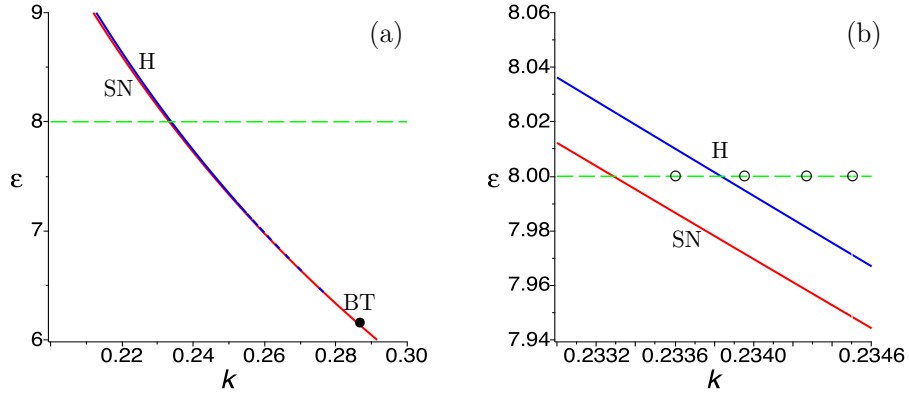


Figure 7: Bifurcation diagram for the codimension-2 B-T bifurcation of the epidemic model (8) with $m=2$, $n=\frac{3}{4}$: (a) a neighborhood of the B-T bifurcation point; and (b) the zoomed area along the line $\varepsilon=8$, marked with four points by circles at $k=0.2336$, 0.23395 , 0.23426542 and 0.2345 .

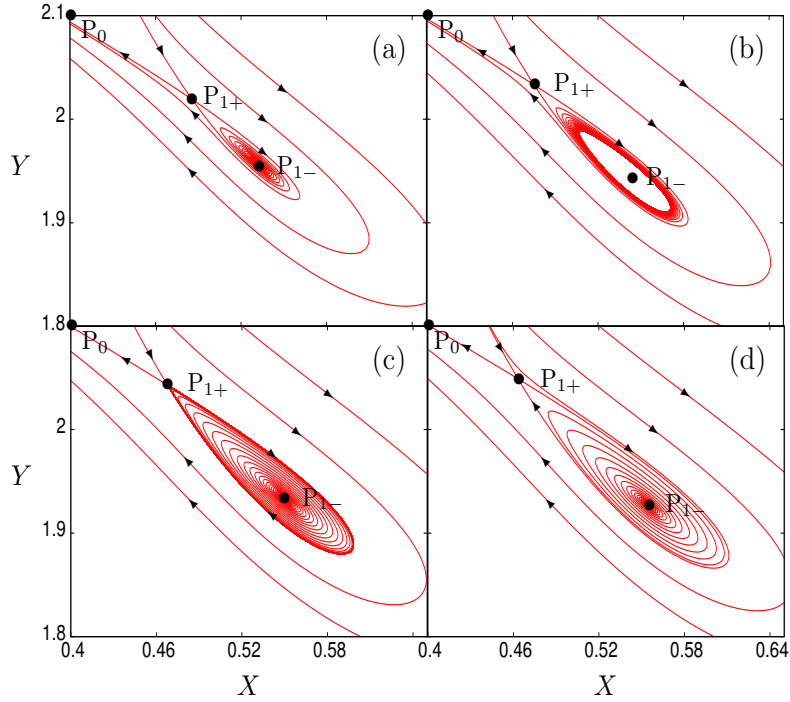


Figure 8: Simulated phase portraits for the codimension-2 B-T bifurcation of the epidemic model (8) with $m=2$, $n=\frac{3}{4}$, and $\varepsilon=8$, for (a) $k=0.2336$ showing the unstable focus P_{1-} , (b) $k=0.23395$ showing Hopf bifurcation yielding an unstable limit cycle and the stable P_{1-} , (c) $k=0.23426542$ showing the unstable homoclinic loop and the stable P_{1-} , and (d) $k=0.2345$ showing the stable focus P_{1-} .

introduce our one-step transformation method.

3.3.1. Summary of the six-step transformation method

In [13], Li *et al.* applied the six-step transformation approach [4] to provide a detailed analysis on the codimension-3 B-T bifurcation of the epidemic model (8). In order to give a comparison, in the following, we first give a brief summary of the result (more details can be found in [13]). The basic idea of this approach is to employ a transformation in each step to remove one or two terms in the Taylor expansion of the vector field, which is not necessarily in algebraic formula and maybe in differential forms. Introducing the following transformation from the critical point,

$$k = \frac{9}{16m} + \mu_1, \quad \varepsilon = \frac{9}{2m} + \mu_2, \quad n = \frac{2m}{9} + \mu_3, \quad x = X - X_1^0, \quad y = Y - Y_1^0,$$

where $X_1^0 = \frac{2m}{9}$, $Y_1^0 = \frac{14m}{9}$, into (8) yields

$$\frac{dx}{d\tau} = -\left(\frac{1}{2} + \mu_3\right)x - y - \frac{14m}{9}\mu_3, \quad \frac{dy}{d\tau} = Q_1(x, y), \quad (43)$$

where Q_1 is a Taylor expansion in x, y and $\mu = (\mu_1, \mu_2, \mu_3)$. To simplify (43), setting $u_1 = x$, $v_1 = -\left(\frac{1}{2} + \mu_3\right)x - y - \frac{14m}{9}\mu_3$ yields

$$\frac{du_1}{d\tau} = v_1, \quad \frac{dv_1}{d\tau} = Q_2(u_1, v_1),$$

where

$$Q_2(u_1, v_1) = \alpha_0 + \alpha_1 u_1 + \alpha_2 v_1 + \alpha_3 u_1 v_1 + a_1 u_1^2 + a_2 v_1^2 + a_3 u_1^3 + a_4 u_1^2 v_1 + a_5 u_1 v_1^2 + a_6 v_1^3,$$

in which α_j 's and a_k 's are parameters, expressed in terms of the coefficients in Q_1 .

Step 1. Use a nonlinear transformation $u_1 = u_2 + \frac{a_0}{2}u_2^2$, $v_1 = v_2 + a_2 u_2 v_2$ to remove the v_1^2 -term from Q_2 , yielding

$$\frac{du_2}{d\tau} = v_2, \quad \frac{dv_2}{d\tau} = Q_3(u_2, v_2) + R(u_2, v_2, \mu),$$

where the residue term R has special property, and

$$Q_3(u_2, v_2) = \beta_0 + \beta_1 u_2 + \beta_2 v_2 + \beta_3 u_2 v_2 + b_1 u_2^2 + b_2 u_2^3 + b_3 u_2^4 + b_4 u_2^2 v_2 + b_5 u_2 v_2^2 + b_6 v_2^3 + b_7 u_2^3 v_2,$$

where β_j 's and b_k 's are parameters, expressed in terms of the coefficients in Q_2 .

Step 2. Use two nonlinear transformations, one in differential form $(u_2, v_2) \rightarrow (u_3, v_3)$ and one in algebraic form $(u_3, v_3) \rightarrow (u_4, v_4)$, to remove the $u_2v_2^2$ - and v_2^3 -terms from Q_3 , resulting in

$$\frac{du_4}{d\tau} = v_4, \quad \frac{dv_4}{d\tau} = Q_5(u_4, v_4) + R(u_4, v_4, \mu).$$

Step 3. Similarly, use a nonlinear transformation $(u_4, v_4) \rightarrow (u_5, v_5)$ to remove the u_4^3 - and u_4^4 -terms from Q_5 , giving

$$\frac{du_5}{d\tau} = v_5, \quad \frac{dv_5}{d\tau} = Q_6(u_5, v_5) + R(u_5, v_5, \mu).$$

Step 4. Applying a nonlinear transformation $(u_5, v_5) \rightarrow (u_6, v_6)$ to remove the $u_5^2v_5$ -term from Q_6 gives

$$\frac{du_6}{d\tau} = v_6, \quad \frac{dv_6}{d\tau} = Q_7(u_6, v_6) + R(u_6, v_6, \mu),$$

where

$$Q_7(u_6, v_6) = \eta_0 + \eta_1 u_6 + \eta_2 v_6 + \eta_3 u_6 v_6 + \tilde{e}_1 u_6^2 + \tilde{e}_3 u_6^3 v_6.$$

Step 5. Normalizing \tilde{e}_1 and \tilde{e}_3 to be 1 in Q_7 yields

$$\frac{du_6}{d\tau} = v_6, \quad \frac{dv_6}{d\tau} = Q_8(u_6, v_6) + R(u_6, v_6, \mu),$$

where

$$Q_8(u_6, v_6) = \sigma_0 + \sigma_1 u_6 + \sigma_2 v_6 + \sigma_3 u_6 v_6 + u_6^2 + u_6^3 v_6.$$

Step 6. Use a nonlinear transformation $(u_6, v_6) \rightarrow (y_1, y_2)$ to remove the u_6 -term from Q_8 , finally yielding the normal form,

$$\begin{aligned} \frac{dy_1}{d\tau} &= y_2, \\ \frac{dy_2}{d\tau} &= \varepsilon_1 + \varepsilon_2 y_2 + \varepsilon_3 y_1 y_2 + y_1^2 + y_1^3 y_2 + R(y_1, y_2, \mu). \end{aligned} \tag{44}$$

A careful checking on the transformations given in [13] we obtain

$$\tilde{e}_1 = \frac{27}{64m}, \quad \tilde{e}_3 = -\frac{3645}{1024m^3}.$$

Moreover, combining the transformations from (μ_1, μ_2, μ_3) to $(\varepsilon_1, \varepsilon_2, \varepsilon_3)$ yields

$$\det \left[\frac{\partial(\mu_1, \mu_2, \mu_3)}{\partial(\varepsilon_1, \varepsilon_2, \varepsilon_3)} \right]_{\mu=0} = -\frac{6}{m^2} \tilde{e}_1^{\frac{12}{5}} \tilde{e}_3^{-\frac{4}{5}} = -\frac{27}{64m^2} \frac{(72)^{\frac{1}{5}}}{5^{\frac{4}{5}}} \neq 0, \tag{45}$$

implying that system (44) with $(\varepsilon_1, \varepsilon_2, \varepsilon_3) \sim (0, 0, 0)$ for (y_1, y_2) near $(0, 0)$ is equivalent to system (8) with $(k, \varepsilon, n) \sim (k_0, \varepsilon_0, n_0)$ for (X, Y) near (X_1^0, Y_1^0) .

It should be pointed out that although the computation demand in each step of the above process is not heavy, finding the complete transformation between the system (8) and the final normal form (44) is not an easy task. Also note that in each of the above transformations, only the dominant terms Q_k are take into account, while the R 's with special property are ignored, which reduces computation demanding.

3.3.2. One-step transformation method

Now, we turn to consider our one-step transformation approach, which is based on the parametric simplest normal form (PSNF) [5, 21, 22]. The main difficulty of this method is how to determine the basis for nonlinear transformations, since different systems require different forms of transformations.

Introducing the transformation,

$$x = x_1^0 + u, \quad y = y_1^0 + v, \quad \kappa = \kappa_0 + \mu_1, \quad e = e_0 + \mu_2, \quad n = n_0 + \mu_3,$$

together with (37) into (11) yields the following system up to 4th order,

$$\begin{aligned} \frac{du}{d\tau} &= v, \\ \frac{dv}{d\tau} &= \frac{16}{27}\mu_1 + \frac{1}{27}\mu_2 + \sum_{i+j+k+l+s=2}^4 p_{ijkl} u^i v^j \mu_1^k \mu_2^l \mu_3^s + \text{h.o.t.}, \end{aligned} \quad (46)$$

where the coefficients p_{ijkl} are real values. Then, applying the change of variables,

$$\begin{aligned} u &= -\frac{4}{9}48^{\frac{1}{5}}y_1 - \frac{1}{6}48^{\frac{2}{5}}\beta_1 + \frac{1}{27}48^{\frac{3}{5}}\beta_2 + \frac{1}{18}48^{\frac{2}{5}}y_1^2 + \frac{1}{9}48^{\frac{2}{5}}y_1y_2 + \frac{1}{240}48^{\frac{3}{5}}y_2^2 \\ &\quad + \left(\frac{763}{2160}48^{\frac{3}{5}}\beta_1 - \frac{8}{81}48^{\frac{4}{5}}\beta_2 + \frac{16}{243}48^{\frac{3}{5}}\beta_3\right)y_1 \\ &\quad + \left(\frac{2386838}{93555}48^{\frac{1}{5}}\beta_1 - \frac{24223}{93555}48^{\frac{2}{5}}\beta_2 + \frac{8306}{5103}48^{\frac{1}{5}}\beta_3\right)y_2 + \frac{103439}{259200}48^{\frac{4}{5}}\beta_1^2 + \frac{22}{81}48^{\frac{1}{5}}\beta_2^2 \\ &\quad - \frac{32}{9}\beta_1\beta_2 + \frac{5}{162}48^{\frac{4}{5}}\beta_1\beta_3 - \frac{32}{243}\beta_2\beta_3 + \sum_{i+j+k+l+s=3}^4 a_{ijkl} y_1^i y_2^j \beta_1^k \beta_2^l \beta_3^s, \\ v &= -\frac{48^{\frac{4}{5}}}{36}y_2 + \frac{7}{54}48^{\frac{3}{5}}y_2^2 + \frac{7}{54}48^{\frac{3}{5}}\beta_1 y_1 + \left(\frac{149}{144}48^{\frac{1}{5}}\beta_1 - \frac{2}{9}48^{\frac{2}{5}}\beta_2 + \frac{2}{27}48^{\frac{1}{5}}\beta_3\right)y_2 \\ &\quad + \frac{1193419}{748440}48^{\frac{4}{5}}\beta_1^2 + \frac{24233}{31185}\beta_1\beta_2 + \frac{4153}{40824}48^{\frac{4}{5}}\beta_1\beta_3 + \sum_{i+j+k+l+s=3}^4 b_{ijkl} y_1^i y_2^j \beta_1^k \beta_2^l \beta_3^s, \end{aligned}$$

where the coefficients b_{ijkl} are real values, the parametrization,

$$\begin{aligned}
\mu_1 &= \frac{9}{64}48^{\frac{2}{5}}\beta_1 + 3108^{\frac{1}{5}}\beta_2 + \frac{15}{128}48^{\frac{4}{5}}\beta_1^2 + \frac{41}{64}48^{\frac{1}{5}}\beta_2^2 - \frac{59}{16}\beta_1\beta_2 \\
&\quad + \frac{11}{384}48^{\frac{4}{5}}\beta_1\beta_3 - \frac{31}{48}\beta_2\beta_3 + \sum_{i+j+k=3}^4 \alpha_{ijk} \beta_1^i \beta_2^j \beta_3^k, \\
\mu_2 &= -972^{\frac{1}{5}}\beta_1 + 3108^{\frac{1}{5}}\beta_2 - 3162^{\frac{1}{5}}\beta_1^2 - 848^{\frac{1}{5}}\beta_2^2 + 38\beta_1\beta_2 \\
&\quad - \frac{13}{3}162^{\frac{1}{5}}\beta_1\beta_3 + \frac{31}{3}\beta_2\beta_3 + \frac{34}{3}162^{\frac{1}{5}}\beta_2^3 - \frac{115}{9}108^{\frac{1}{5}}\beta_2^2\beta_3 + \frac{25}{6}72^{\frac{1}{5}}\beta_2\beta_3^2, \\
\mu_3 &= \frac{5}{12}72^{\frac{1}{5}}\beta_1 - \frac{1}{4}108^{\frac{1}{5}}\beta_2 - \frac{1645571}{51840}162^{\frac{1}{5}}\beta_1^2 + \frac{1}{6}48^{\frac{1}{5}}\beta_2^2 + \frac{2}{81}162^{\frac{1}{5}}\beta_3^2 \\
&\quad - \frac{9119}{1800}\beta_1\beta_2 - \frac{31}{810}162^{\frac{1}{5}}\beta_1\beta_3 - \frac{1}{3}\beta_2\beta_3,
\end{aligned}$$

and the time rescaling,

$$d\tau = \left(\frac{1}{4}108^{\frac{1}{5}} - \frac{1}{4}162^{\frac{1}{5}}y_1 - \frac{1}{6}48^{\frac{1}{5}}\beta_2 + \frac{5}{18}\beta_3 \right) d\tau_1,$$

into (46) yields the following PSNF up to 4th-order terms,

$$\begin{aligned}
\frac{dy_1}{d\tau_1} &= y_2, \\
\frac{dy_2}{d\tau_1} &= \beta_1 + \beta_2 y_2 + \beta_3 y_1 y_2 + y_1^2 + y_1^3 y_2 + \mathcal{O}(|(y_1, y_2, \beta)|^5).
\end{aligned} \tag{47}$$

It is easy to verify that

$$\det \left[\frac{\partial(\mu_1, \mu_2, \mu_3)}{\partial(\beta_1, \beta_2, \beta_3)} \right]_{\beta=0} = -\frac{27}{64}72^{\frac{1}{5}} \neq 0, \tag{48}$$

which shows that near the critical point $\mu = 0$, system (8) has the same bifurcation set with respect to μ as system (47) has that with respect to β , up to a homeomorphism in the parameter space.

Comparing our one-step transformation method with the classical six-step transformation approach, we have the following observations.

- (i) The one-step approach depends upon purely algebraic computation; while the six-step approach involves different types of transformations.
- (ii) The one-step approach yields a direct relation between the SNF (or PSNF) and the original system, which makes it convenient in applications; while for the six-step approach, finding a direct relation needs to put all the transformation together, which involves a lot of computations.

- (iii) The one-step approach is easier to be used for developing a general algorithm for the symbolic computation.
- (iv) The one-step approach provides a complete nonlinear transformation up to a given order, while the six-step approach only take the dominant parts in each step of transformation.
- (v) The six-step approach has less computation in each step; while the computation demands for the one-step is higher, in particular for higher-codimension bifurcations.

Now, following the method described in [4], and the computations in [22], we apply the method of normal forms and Abelian integral (or the Melnikov function method) to derive the bifurcations for the codimension-3 B-T bifurcation. In [22], the term $x_1^3 x_2$ (same as $y_1^3 y_2$ in (47)) in the normal form has a coefficient $-b_1$. So, theoretically speaking, we can use the formulas in [22] and set $b_1 = -1$ to directly obtain the bifurcation results for our system (47). However, it has been noted that there are some errors in the formulas given in [22] for the codimension-3 B-T bifurcation, as listed below.

- (a) In Eqn. (91), $\xi_3 + 3b_1\xi_1$ should be $\xi_3 - 3b_1\xi_1$.
- (b) In Eqn. (93), $\frac{103}{55}$ should be $\frac{179}{11}$.
- (c) In Eqn. (107), $z_1(t) = -3 \operatorname{sech}^2(t)$ and $z_2(t) = 3 \operatorname{sech}^2(t) \tanh(t)$ should be $z_1(t) = -3 \bar{\nu}_1 \operatorname{sech}^2(t)$ and $z_2(t) = 3 \bar{\nu}_1 \operatorname{sech}^2(t) \tanh(t)$, respectively, and thus $-\frac{103}{77}$ should be $\frac{895}{77}$.
- (d) In Eqn. (109), $\frac{103}{55}$ should be $\frac{179}{11}$.

Then, other changes in Eqns. (112)-(115) are followed accordingly. However, note that the bifurcation results shown in Figure 19 of [22] are qualitatively not changed.

In order to correct the errors in [22] and provide readability for readers, in the following we briefly describe the derivations. First of all, it is easy to see that system (47) has two equilibrium solutions E_{\pm} ,

$$\tilde{E}_{\pm} = (y_{1\pm}, 0), \quad \text{where } y_{1\pm} = \pm\sqrt{-\beta_1} \quad \text{for } \beta_1 < 0. \quad (49)$$

The Jacobian of (47) evaluated at \tilde{E}_{\pm} is given by

$$J_{\pm} = \begin{bmatrix} 0 & 1 \\ 2y_{1\pm} & \beta_2 + \beta_3 y_{1\pm} + y_{1\pm}^3 \end{bmatrix},$$

which indicates that \tilde{E}_+ is a saddle, and \tilde{E}_- is either a focus or node. It is easy to see from the Jacobian that the plane

$$\text{SN} = \{(\beta_1, \beta_2, \beta_3) \mid \beta_1 = 0\}, \quad (50)$$

excluding the origin in the parameter space is the saddle-node bifurcation surface. Hopf bifurcation occurs from \tilde{E}_- on the critical surface, defined by that the trace equals zero, i.e.,

$$\beta_2 - (\beta_3 - \beta_1)\sqrt{-\beta_1} = 0, \quad (\beta_1 < 0).$$

Based on Hopf bifurcation theory, a direct computation (e.g., with the Maple program in [19]) yields the following focus values,

$$v_1 = \frac{\beta_3 + 3\beta_1}{16\sqrt{-\beta_1}} \quad \text{and} \quad v_2|_{v_1=0} = \frac{5}{96\sqrt{-\beta_1}} > 0,$$

which implies that generalized Hopf bifurcation occurs on the surface, defined by $v_1 = 0$,

$$\beta_3 + 3\beta_1 = 0, \quad (\beta_1 < 0), \quad (51)$$

leading to two limit cycles, with the outer one unstable and the inner one stable, and both of them enclose the unstable focus \tilde{E}_- .

Next, to find the homoclinic and the degenerate homoclinic bifurcations, we apply the Melnikov function method [11]. Introducing the scaling,

$$y_1 = \varepsilon^{\frac{2}{5}}w_1, \quad y_2 = \varepsilon^{\frac{3}{5}}w_2, \quad \beta_1 = \varepsilon^{\frac{4}{5}}\varphi_1, \quad \beta_2 = \varepsilon^{\frac{6}{5}}\varphi_2, \quad \beta_3 = \varepsilon^{\frac{4}{5}}\varphi_3, \quad \tau_2 = \varepsilon^{\frac{1}{5}}\tau_1, \quad (0 < \varepsilon \ll 1),$$

together with the following transformation,

$$w_1 = \bar{\varphi}_1 + \tilde{x}_1, \quad w_2 = \sqrt{2\bar{\varphi}_1}\tilde{x}_2, \quad \tau_3 = \sqrt{2\bar{\varphi}_1}\tau_2, \quad \varphi_1 = -\bar{\varphi}_1^2, \quad (\bar{\varphi}_1 > 0),$$

into (47) we obtain

$$\begin{aligned} \frac{d\tilde{x}_1}{d\tau_3} &= \tilde{x}_2, \\ \frac{d\tilde{x}_2}{d\tau_3} &= \tilde{x}_1 + \frac{1}{2\bar{\varphi}_1}\tilde{x}_1^2 + \varepsilon q(\tilde{x}_1, \tilde{x}_2, \bar{\varphi}), \end{aligned} \quad (52)$$

where

$$q(\tilde{x}_1, \tilde{x}_2, \bar{\varphi}) = \frac{1}{\sqrt{2\bar{\varphi}_1}} [(\varphi_2 + \bar{\varphi}_1\varphi_3 + \bar{\varphi}_1^3)\tilde{x}_2 + (\varphi_3 + 3\bar{\varphi}_1^2)\tilde{x}_1\tilde{x}_2 + 3\bar{\varphi}_1\tilde{x}_1^2\tilde{x}_2 + \tilde{x}_1^3\tilde{x}_2],$$

with $\bar{\varphi} = (\bar{\varphi}_1, \varphi_2, \varphi_3)$.

The system (52)| $_{\varepsilon=0}$ is a Hamiltonian system with two equilibrium solutions,

$$\bar{E}_- = (-2\bar{\varphi}_1, 0) \quad \text{and} \quad \bar{E}_0 = (0, 0),$$

with \bar{E}_- and \bar{E}_0 being center and saddle, respectively. These two equilibria correspond to the \tilde{E}_\pm defined in (49). The Hamiltonian is given by

$$H(\tilde{x}_1, \tilde{x}_2) = \frac{1}{2} (\tilde{x}_2^2 - \tilde{x}_1^2) - \frac{1}{6\bar{\varphi}_1} \tilde{x}_1^3,$$

and the homoclinic orbit connecting E_0 is described by

$$\Gamma_0 : \quad H(\tilde{x}_1, \tilde{x}_2) = \frac{1}{2} (\tilde{x}_2^2 - \tilde{x}_1^2) - \frac{1}{6\bar{\varphi}_1} \tilde{x}_1^3, \quad \text{with } H(0, 0) = 0,$$

and $H(-2\bar{\varphi}_1, 0) = -\frac{2}{3}\bar{\varphi}_1^2$. Thus, any closed orbits of the Hamiltonian system (52)| $_{\varepsilon=0}$ inside Γ_0 can be described by

$$\Gamma_h : \quad H(\tilde{x}_1, \tilde{x}_2, h) = \frac{1}{2} (\tilde{x}_2^2 - \tilde{x}_1^2) - \frac{1}{6\bar{\varphi}_1} \tilde{x}_1^3 - h = 0, \quad h \in \left(-\frac{2}{3}\bar{\varphi}_1^2, 0\right).$$

Now, the Abelian integral or the (first-order) Melnikov function for the perturbed system (52) can be written as [11]

$$\begin{aligned} M(h, \varphi) &= \oint_{\Gamma_h} [q(\tilde{x}_1, \tilde{x}_2, \varphi) d\tilde{x}_1 - p(\tilde{x}_1, \tilde{x}_2, \varphi) d\tilde{x}_2]_{\varepsilon=0} \quad (p = 0) \\ &= \oint_{\Gamma_h} q(\tilde{x}_1, \tilde{x}_2, \varphi)|_{\varepsilon=0} d\tilde{x}_1 = \oint_{\Gamma_h} H_{\tilde{x}_2} q(\tilde{x}_1, \tilde{x}_2, \varphi)|_{\varepsilon=0} d\tau_3 \\ &= \frac{1}{\sqrt{2\bar{\varphi}_1}} \oint_{\Gamma_h} \tilde{x}_2^2 [\varphi_2 + \bar{\varphi}_1 \varphi_3 + \bar{\varphi}_1^3 + (\varphi_3 + 3\bar{\varphi}_1^2)\tilde{x}_1 + 3\bar{\varphi}_1 \tilde{x}_1^2 + \tilde{x}_1^3] d\tau_3 \\ &= C_0(\varphi) + C_1(\varphi) h \ln |h| + C_2(\varphi) h + C_3(h) h^2 \ln |h| + \dots, \end{aligned}$$

for $0 < -h \ll 1$, where

$$\begin{aligned} C_0(\varphi) &= \frac{1}{\sqrt{2\bar{\varphi}_1}} \oint_{\Gamma_0} \tilde{x}_2^2 [\varphi_2 + \bar{\varphi}_1 \varphi_3 + \bar{\varphi}_1^3 + (\varphi_3 + 3\bar{\varphi}_1^2)\tilde{x}_1 + 3\bar{\varphi}_1 \tilde{x}_1^2 + \tilde{x}_1^3] d\tau_3, \\ C_1(\varphi) &= a_{10} + b_{01}, \end{aligned}$$

in which a_{10} and b_{01} are the coefficients in the functions $p(\tilde{x}_1, \tilde{x}_2, \varphi)$ and $q(\tilde{x}_1, \tilde{x}_2, \varphi)$, given by

$$a_{10} = 0, \quad b_{01} = \frac{1}{\sqrt{2\bar{\varphi}_1}} (\varphi_2 + \bar{\varphi}_1 \varphi_3 + \bar{\varphi}_1^3).$$

To compute $C_0(\varphi)$, introducing the parametric transformation,

$$\tilde{x}_1(\tau_3) = -3\bar{\varphi}_1 \operatorname{sech}^2(\tau_3), \quad \tilde{x}_2(\tau_3) = 3\bar{\varphi}_1 \operatorname{sech}^2(\tau_3) \tanh(\tau_3),$$

into $C_0(\varphi)$ with a direct integration we obtain

$$C_0(\varphi) = \frac{6\bar{\varphi}_1\sqrt{2\bar{\varphi}_1}}{5} \left(\varphi_2 - \frac{5}{7}\bar{\varphi}_1\varphi_3 - \frac{895}{77}b_1\bar{\varphi}_1^3 \right).$$

Finally, we express $C_0(\varphi)$ and $C_1(\varphi)$ in terms of the original perturbation parameters β_j by using

$$\bar{\varphi}_1 = \sqrt{-\varphi_1} = \sqrt{-\varepsilon^{-\frac{4}{5}}\beta_1} = \varepsilon^{-\frac{2}{5}}\sqrt{-\beta_1}, \quad \varphi_2 = \varepsilon^{-\frac{6}{5}}\beta_2, \quad \varphi_3 = \varepsilon^{-\frac{4}{5}}\beta_3,$$

as

$$\begin{aligned} C_0(\beta) &= \frac{6\bar{\varphi}_1\sqrt{2\bar{\varphi}_1}}{5} \varepsilon^{-\frac{6}{5}} \left[\beta_2 - \frac{5}{7} \left(\beta_3 - \frac{179}{11}\beta_1 \right) \sqrt{-\beta_1} \right], \\ C_1(\beta) &= \frac{1}{\sqrt{2\bar{\varphi}_1}} \varepsilon^{-\frac{6}{5}} \left[\beta_2 + (\beta_3 - \beta_1)\sqrt{-\beta_1} \right]. \end{aligned} \tag{53}$$

Hence, the homoclinic and degenerate homoclinic bifurcation surfaces are defined by $C_0(\beta)=0$ and $C_1(\beta)=0$, respectively.

Summarizing the above results we obtain the following theorem. Note that a summary of the result was given in [13]. Here, more detailed formulas are provided.

Theorem 3.3. *For the epideminc model (11), codimension-3 B-T bifurcation occurs from the equilibrium $P_1: (x, y) = (\frac{2}{9}, \frac{14}{9})$ when $\kappa = \frac{9}{16}$, $e = \frac{9}{2}$ and $n = \frac{1}{2}$. Moreover, six local bifurcations with the representations of the bifurcation surfaces/curves are obtained, as given below.*

(1) *Saddle-node bifurcation occurs from the critical surface:*

$$\text{SN} = \{(\beta_1, \beta_2, \beta_3) \mid \beta_1 = 0\}.$$

(2) *Hopf bifurcation occurs from the critical surface:*

$$\text{H} = \{(\beta_1, \beta_2, \beta_3) \mid \beta_1 < 0, \beta_2 = (\beta_3 - \beta_1)\sqrt{-\beta_1}\}.$$

(3) *Homoclinic loop bifurcation occurs from the critical surface:*

$$\text{HL} = \{(\beta_1, \beta_2, \beta_3) \mid \beta_1 < 0, \beta_2 = \frac{5}{7}(\beta_3 - \frac{179}{11}\beta_1)\sqrt{-\beta_1}\}.$$

(4) *Generalized Hopf bifurcation occurs from the critical curve:*

$$\text{GH} = \left\{ (\beta_1, \beta_2, \beta_3) \mid \beta_1 < 0, \beta_2 = -4\beta_1\sqrt{-\beta_1}, \beta_3 = -3\beta_1 \right\}.$$

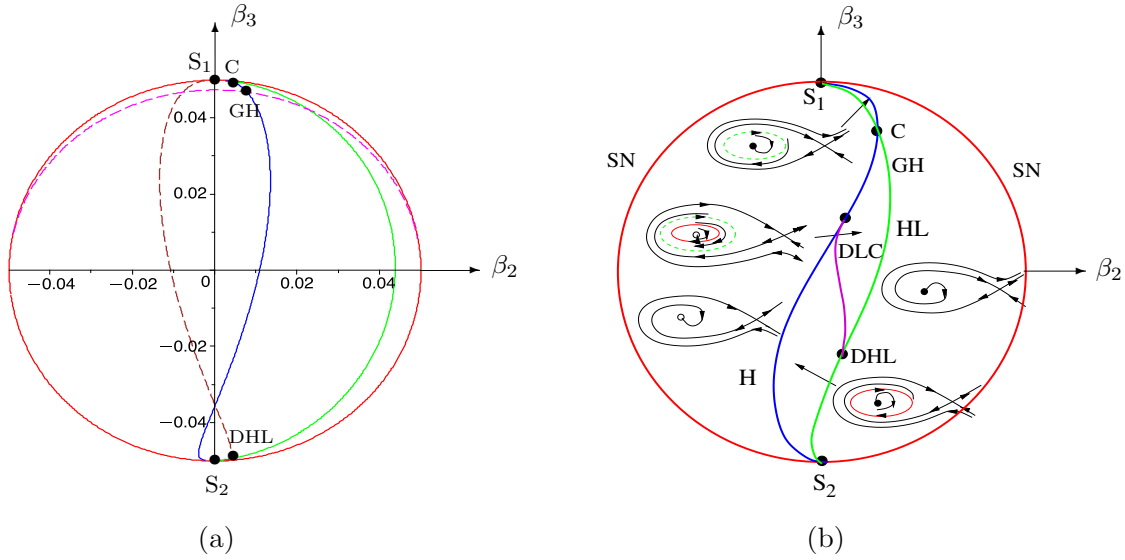


Figure 9: Bifurcation diagram for the codimension-3 B-T bifurcation based on the normal form (47), displayed in the intersection of the cone and the 2-sphere $\beta_1^2 + \beta_2^2 + \beta_3^2 = \sigma^2$, with the red color curve for saddle-node, blue curve for Hopf and green curve for homoclinic loop bifurcations, respectively: (a) with $\sigma=0.05$, where the intersection point of the pink and blue curves is the degenerate Hopf bifurcation, and the intersection point of the brown and green curves denotes the degenerate homoclinic loop bifurcation; and (b) a schematic bifurcation diagram, where the GH and DHL represent the generalized Hopf critical point and the degenerate homoclinic critical point, respectively.

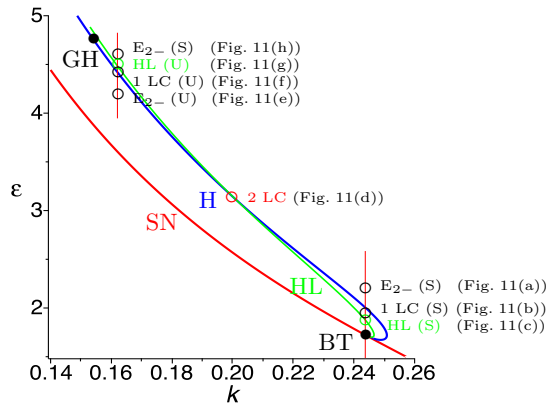


Figure 10: Bifurcation diagram for the codimension-3 B-T bifurcation of the epidemic model (8) with $m=2$, $n = \frac{5}{12}$, in the parameter k - ϵ space, with the red, blue and green curves (obtained from numerical computation) representing the saddle-node (SN), Hopf (H) and homoclinic loop (HL) bifurcations, respectively, and the blank circles indicate the parameter values for simulations, which are given in Figure 11.

(5) *Degenerate homoclinic bifurcation occurs from the critical curve:*

$$\text{DHL} = \{(\beta_1, \beta_2, \beta_3) \mid \beta_1 < 0, \beta_2 = -\frac{70}{11} \beta_1 \sqrt{-\beta_1}, \beta_3 = \frac{81}{11} \beta_1\}.$$

(6) *Double limit cycle bifurcation occurs from a critical surface, which is tangent to the Hopf bifurcation surface H on the critical curve GH, and tangent to the homoclinic bifurcation surface HL on the critical curve DHL.*

The bifurcation diagram projected on a 2-sphere is shown in Figure 9. Figure 9(a) is an exact bifurcation diagram for $\sigma = 0.05$, in which the intersection points C, GH and DHL, as shown in Figure 9(a), are given by

$$\begin{aligned} \text{C} &= (\beta_2, \beta_3)_{\text{C}} = (0.001880, 0.049947), & \text{for } \beta_1 &= -0.001343, \\ \text{GH} &= (\beta_2, \beta_3)_{\text{GH}} = (0.007807, 0.046852), & \text{for } \beta_1 &= -0.015617, \\ \text{DHL} &= (\beta_2, \beta_3)_{\text{DHL}} = (0.003499, -0.049424), & \text{for } \beta_1 &= -0.006712. \end{aligned}$$

For a better view of bifurcations, a schematic general bifurcation diagram is shown in Fig. 9(b) with typical phase portraits, which is similar to Figure 3 in [4] and Figure 2 in [13].

Finally, we present the simulation for the codimension-3 B-T bifurcation to show the dynamics described in Theorem 3.3. For convenience, we use the model (8) to plot the bifurcation diagram in the k - ε plane. For this purpose, we take $m = 2$, and $\mu_3 = -\frac{1}{12}$, yielding

$$n = n_0 + \mu_3 = \frac{1}{2} - \frac{1}{12} = \frac{5}{12}.$$

Then, the bifurcation diagram plotted in the k - ε space, is shown in Figure 10, where the red, blue and green curves represent the saddle-node, Hopf and homoclinic loop bifurcations, respectively. The green curve for the homoclinic loop bifurcation is obtained from numerical computation. It is seen that the bifurcation diagram in Figure 10 agrees well with those in Figure 9, but in a reflection matter, namely, the stable equilibrium E_{2-} in Figure 10 appears on the right side of the Hopf bifurcation curve, while it is on the left side of Hopf bifurcation curve in Figure 9. The eight blank circles in Figure 10 indicate the points of (k, ε) parameter values for simulation, which, except for the red circle point yielding 2 limit cycles, are located on the two lines: $k = 0.16202$ and $k = 0.2439$. Note that the red circle point, $(k, \varepsilon) = (0.2, 3.13)$ for the 2 limit cycles, is below both the blue (H) and green (HL) curves, since at $k = 0.2$, $\varepsilon = 3.14402$ and $\varepsilon = 3.14519$ on the Hopf and homoclinic loop curves, respectively. The two green circles (on the

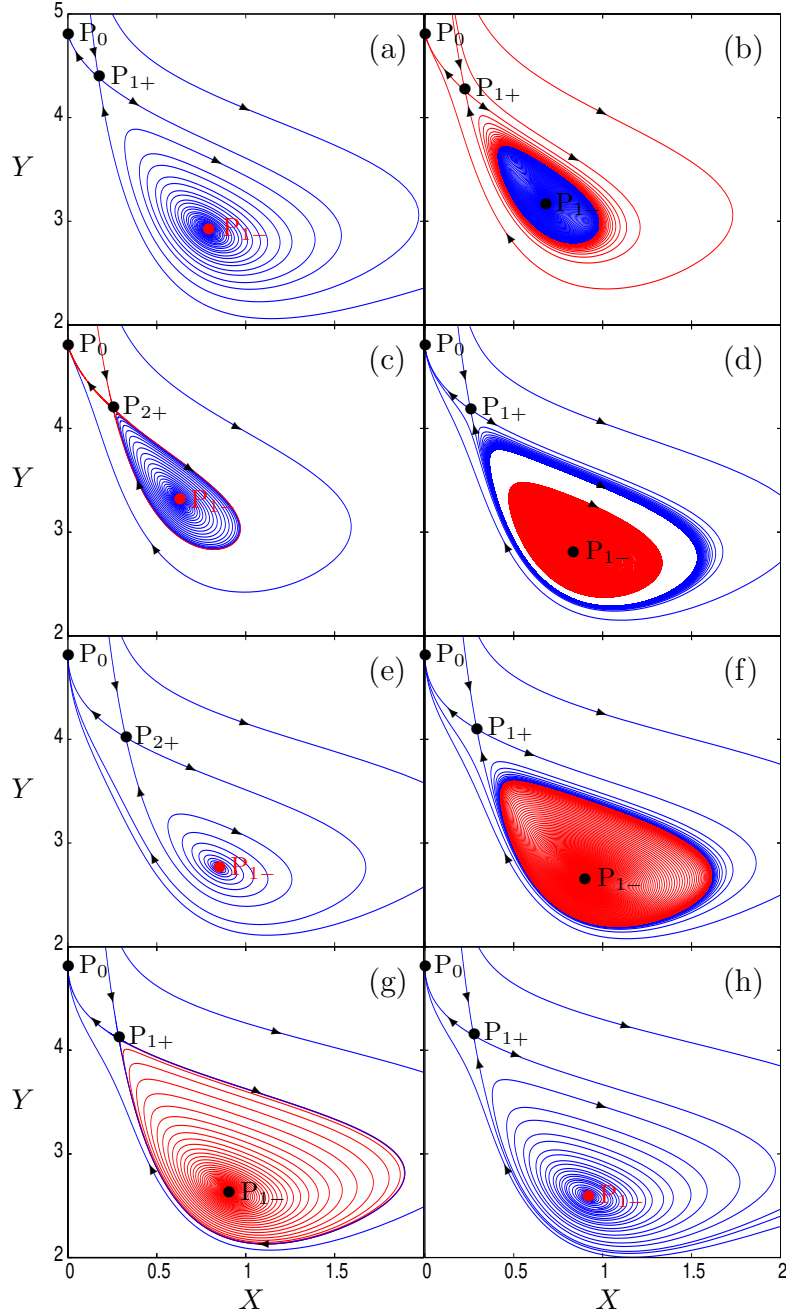


Figure 11: Simulated trajectories for the epidemic model (8) with $m=2$, $n=\frac{5}{12}$, showing the bifurcations given in Figure 10: (a) the stable P_{1-} for $(k, \varepsilon) = (0.2439, 2.2)$; (b) a stable LC for $(k, \varepsilon) = (0.2439, 1.95)$; (c) the stable HL for $(k, \varepsilon) = (0.2439, 1.871268)$; (d) 2 LC for $(k, \varepsilon) = (0.2, 3.13)$; (e) the unstable E_{2-} for $(k, \varepsilon) = (0.16202, 4.2)$; (f) an unstable LC for $(k, \varepsilon) = (0.16202, 4.44)$; (g) the unstable HL for $(k, \varepsilon) = (0.16202, 4.485125)$; and (h) the stable E_{2-} for $(k, \varepsilon) = (0.16202, 4.6)$, where LC and HL represent limit cycle and homoclinic loop, respectively.

green curves) denote the two homoclinic loop bifurcations, with the right one (on the line $k = 0.2439$) stable and the left one (on the line $k = 0.16202$) unstable. Therefore, starting from the points on the line $k = 0.2439$ (in the downward direction) to the 2-LC point, and then to the points on the line $k = 0.16202$ (in the upward direction), we obtain the corresponding simulation figures depicted in Figure 11, as indicated in Figure 10, which indeed, with a careful selection of the parameter values, demonstrates the complex bifurcation behaviours around the codimension-3 B-T bifurcation point.

4. Conclusion

In this paper, we have studied Hopf and Bogdanov-Takens bifurcations and paid particular attention to the codimension of the two bifurcations as well as to the dynamical behaviours around the bifurcation points. We have used an epidemic model to illustrate how to determine the codimension of Hopf and Bogdanov-Takens bifurcations. It has been shown that the difficulty mainly comes from the restriction on the system parameters. Moreover, for the codimension-3 Bogdanov-Takens bifurcation, we have introduced the one-step transformation approach, showing the advantage of this method compared to the classical six-step transformation approach. Numerical simulations are presented to show an excellent agreement with the theoretical predictions.

Acknowledgement

This research was partially supported by the Natural Sciences and Engineering Research Council of Canada (NSERC No. R2686A02).

References

- [1] A. Algaba, E. Freire, E. Gamero, Hypernormal form for the Hopf-zero bifurcation, *Int. J. Bifurcation and Chaos* 8 (1998) 1857–1887. <https://doi.org/10.1142/S0218127498001583>.
- [2] A. Baider and J. A. Sanders, Unique normal forms: the nilpotent Hamiltonian case, *J. Differ. Equ.* 92 (1991) 282–304. [https://doi.org/10.1016/0022-0396\(91\)90050-J](https://doi.org/10.1016/0022-0396(91)90050-J).
- [3] A. Dhooge, W. Govaerts, Yu. A. Kuznetsov, MATCONT: A MATLAB package for numerical bifurcation analysis of ODEs, *ACM Trans. Math. Software*, 29 (2003) 141–164. <https://doi.org/10.1145/779359.779362>.

- [4] F. Dumortier, R. Roussarie, J. Sotomayor, Generic 3-parameter families of vector fields on the plane, unfolding a singularity with nilpotent linear part. The cusp case of codimension 3, *Ergodic Theory Dynam. Systems* 7 (1987) 375–413. <https://doi.org/10.1017/S0143385700004119>.
- [5] M. Gazor, M. Moazeni, Parametric normal forms for Bogdanov-Takens singularity; the generalized saddle-node case, *Discrete Contin. Dyn. Syst. Ser. A* 35 (2015) 205–224. <https://doi.org/10.48550/arXiv.1304.7329>.
- [6] M. Gazor, P. Yu, Formal decomposition method and parametric normal form, *Int. J. Bifurcation and Chaos* 20 (2010) 3487–3415. <https://doi.org/10.1142/S0218127410027830>.
- [7] M. Gazor, P. Yu, Spectral sequences and parametric normal forms, *J. Differ. Equ.* 252 (2012) 1003–1031. <https://doi.org/10.1016/j.jde.2011.09.043>.
- [8] J. Guckenheimer, P. Holmes, *Nonlinear Oscillations, Dynamical Systems, and Bifurcations of Vector Fields*, fourth ed., Springer, New York, 1993.
- [9] M. Han, Bifurcation of limit cycles and the cusp of order n , *Acta Math. Sinica* 13 (1997) 64–75. <https://doi.org/10.1007/BF02560525>.
- [10] M. Han, J. Llibre, J. Yang, On uniqueness of limit cycles in general Bogdanov–Takens bifurcation, *Int. J. Bifurcation and Chaos* 28 (2018) 1850115 (12 pages). <https://doi.org/10.1142/S0218127418501158>.
- [11] M. Han, P. Yu, *Normal Forms, Melnikov Functions, and Bifurcations of Limit Cycles*, Springer-Verlag, London, 2012.
- [12] Yu. A. Kuznetsov, *Elements of Applied Bifurcation Theory*, second ed., Springer, New York, 1998.
- [13] C. Li, J. Li, Z. Ma, Codimension 3 B-T bifurcations in an epidemic model with a nonlinear incidence, *Discrete Contin. Dyn. Syst. Ser. B* 20 (2015) 1107–1116. <https://doi.org/10.3934/dcdsb.2015.20.1107>.
- [14] J. Li, Y. Zhou, J. Wu, Z. Ma, Complex dynamics of a simple epidemic model with a nonlinear incidence, *Discrete Contin. Dyn. Syst. Ser. B* 8 (2007) 161–173. <https://doi.org/10.3934/dcdsb.2007.8.161>.

- [15] J. E. Marsden, M. McCracken, *The Hopf bifurcation and Its Applications*, Springer-Verlag, New York, 1976.
- [16] M.R. Roussel, *Nonlinear Dynamics - A Hands-On Introductory Survey*, Morgan and Claypool, San Rafael, California, 2019
- [17] F. Takens, Singularities of vector fields, *Publ. Math. IHES* 43 (1974) 47–100. <https://doi.org/10.1007/BF02684366>.
- [18] S. Ushiki, Normal forms for singularities of vector fields, *Japan J. Appl. Math.* 1 (1984) 1–37. <https://doi.org/10.1007/BF03167860>.
- [19] P. Yu, Computation of normal forms via a perturbation technique, *J. Sound Vib.* 211 (1998) 19–38. <https://doi.org/10.1006/jsvi.1997.1347>.
- [20] P. Yu, Simplest normal forms of Hopf and generalized Hopf bifurcations, *Int. J. Bifurcation and Chaos* 9 (1999) 1917–1939. <https://doi.org/10.1142/S0218127499001401>.
- [21] P. Yu, A. Y. L. Leung, The simplest normal form of Hopf bifurcation, *Nonlinearity* 16 (2003) 277–300. <https://doi.org/10.1088/0951-7715/16/1/317>.
- [22] P. Yu, W. Zhang, Complex dynamics in a unified SIR and HIV disease model: A bifurcation theory approach, *J. Nonlinear Sci.* 29 (2019) 2447–2500. <https://doi.org/10.1007/s00332-019-09550-7>.
- [23] B. Zeng, S. Deng, P. Yu, Bogdanov-Takens bifurcation in predator-prey systems, *Discrete Contin. Dyn. Syst. Ser. S* 13 (2020) 3253–3269. <https://doi.org/10.3934/dcdss.2020130>.
- [24] B. Zeng, P. Yu, A hierarchical parametric analysis on Hopf bifurcation of an epidemic model, *Discrete Contin. Dyn. Syst. Ser. S* (2022) (online since March 23, 2022). <https://doi.org/10.3934/dcdss.2022069>.